

Sensitivity of future Continental United States water deficit projections to General Circulation Model, evapotranspiration estimation method, and greenhouse gas emission scenario

S. Chang¹, W. Graham^{1, 2}, S. Hwang³, and R. Muñoz-Carpena⁴

[1] Department of Agricultural and Biological Engineering, University of Florida, 570 Weil Hall, PO Box 116601, Gainesville, FL 32611, USA

[2] Water Institute, University of Florida, 570 Weil Hall, PO Box 116601, Gainesville, FL 32611, USA

[3] Department of Agricultural Engineering, Institute of Agriculture and Life Science, Gyeongsang National University, Jinju, 660-701, South Korea

[4] Department of Agricultural and Biological Engineering, University of Florida, 287 Frazier Rogers Hall, PO Box 110570, Gainesville, FL 32611, USA

Correspondence to: W. Graham (wgraham@ufl.edu)

Abstract

Projecting water deficit under various possible future climate scenarios depends on the choice of General Circulation Model (GCM), reference evapotranspiration (ET_0) estimation method and Representative Concentration Pathway (RCP) trajectory. The relative contribution of each of these factors must be evaluated in order to choose an appropriate ensemble of future scenarios for water resources planning. In this study variance-based global sensitivity analysis and Monte Carlo filtering were used to evaluate the relative sensitivity of projected changes in precipitation (P), ET_0 and water deficit (defined here as $P - ET_0$) to choice of GCM, ET_0 estimation method and RCP trajectory over the continental United States (US) for two distinct future periods: 2030-2060 (future period 1) and 2070-2100 (future period 2). A total of 9 GCMs, 10 ET_0 methods and 3 RCP trajectories were used to quantify the range of future projections and

27 estimate the relative sensitivity of future projections to each of these factors. In general, for all
28 regions of the Continental US, changes in future precipitation are most sensitive to the choice of
29 GCM, while changes in future ET_0 are most sensitive to the choice of ET_0 estimation method.
30 For changes in future water deficit, the choice of GCM is the most influential factor in the cool
31 season (Dec – Mar) and the choice of ET_0 estimation method is most important in the warm
32 season (May – Oct) for all regions except the South East US where GCM and ET_0 have
33 approximately equal influence throughout most of the year. Although the choice of RCP
34 trajectory is generally less important than the choice of GCM or ET_0 method, the impact of RCP
35 trajectory increases in future period 2 over future period 1 for all factors. Monte Carlo filtering
36 results indicate that particular GCMs and ET_0 methods drive the projection of wetter or drier
37 future conditions much more than RCP trajectory; however the set of GCMs and ET_0 methods
38 that produce wetter or drier projections varies substantially by region. Results of this study
39 indicate that, in addition to using an ensemble of GCMs and several RCP trajectories, a range of
40 regionally-relevant ET_0 estimation methods should be used to develop a robust range of future
41 conditions for water resource planning under climate change.

42

43 **1. Introduction**

44 Climate change will result in significant impacts on hydrologic processes. The 2014 Fifth
45 Assessment Report (AR5) of the Intergovernmental Panel on Climate Change (IPCC) reported
46 that climate change will significantly affect future precipitation (P), temperature (T) and
47 reference evapotranspiration (ET_0) and these changes will affect the quantity and quality of water
48 resources. The most recent report of the National Climate Assessment and Development
49 Advisory Committee (NCADAC, 2013) indicated that the average annual temperature in the
50 United States (US) has increased by 0.7 °C to 0.9 °C since record keeping began in 1895 and is
51 expected to continue to rise (Georgakakos et al., 2014; Walsh et al., 2014). The NCADAC report
52 also indicated that Coupled Model Intercomparison Project 5 (CMIP5) General Circulation
53 Model (GCM) precipitation projections show a consistent increase in Alaska and the far north of
54 the continental US and a consistent decrease in the far Southwest US, but that GCM projections
55 are inconsistent in the precipitation transition zone of the US continent. The uncertainty in
56 climate change projections makes actionable water resources planning difficult in many regions.

57 In order to predict changes in the hydrologic cycle, and future water supply and demand,
58 estimates of changes in P, T and ET_0 must be evaluated on a regional basis, and the uncertainty
59 of these estimates must be quantified (Ishak et al., 2010).

60 Previous research has evaluated existing and potential future spatiotemporal changes in P,
61 T and ET_0 for various regions around the globe (e.g. Chaouche et al., 2010; Chong-Hai and
62 Ying, 2012; Johnson and Sharma, 2009; Kharin et al., 2013; Maurer and Hidalgo, 2008;
63 Quintana Seguí et al., 2010; Sung et al., 2012; Thomas, 2000; Wang et al., 2013; Xu et al.,
64 2006). It is well known that future GCM projections of temperature and precipitation vary
65 significantly due to both the different radiative forcing assumptions of carbon dioxide scenarios
66 (e.g. CMIP3 Special Report on Emissions Scenarios (SRES) and CMIP5 Representative
67 Concentration Pathways (RCP trajectories)) and different GCM model physics (Hawkins and
68 Sutton, 2009, 2010). Future ET_0 projections have been shown to depend on ET_0 estimation
69 methods in addition to GCMs. For example, Wang et al. (2015) used projections from the
70 CMIP3 HADCM3 model A2 scenario and found that the physically-based Penman-Monteith
71 equation, which uses less reliable GCM projection data (including vapor pressure and solar
72 radiation), and the empirical temperature-based Hargreaves equation showed similar patterns but
73 different magnitudes for future ET_0 changes over the Hanjiang River Basin in China. Kingston et
74 al. (2009) used 5 GCMs from the CMIP3 climate projections and 6 different ET_0 equations to
75 estimate global ET_0 and found that the choice of ET_0 method contributes to different projections
76 of the future state of water resources which varies by region. They found that the Hamon and
77 Jensen-Haise ET_0 estimates showed the greatest changes in both humid and arid regions while
78 the Penman-Monteith and Priestley-Taylor estimates frequently showed smallest change.
79 Similarly McAfee (2013) used three ET_0 equations with 17 CMIP3 GCMs to evaluate the
80 uncertainty of future global ET_0 projections and found that the Hamon equation showed more
81 significant and consistently positive trends in ET_0 compared to the Priestley-Taylor and Penman
82 methods.

83 Models developed to estimate future water supply and demand as a result of projected
84 climate change use many different types of ET_0 estimation methods (Zhao et al., 2013). Because
85 the choice of ET_0 estimation method may be as important as the choice of GCM or RCP
86 trajectory, better understanding of the contribution of each of these factors to the overall

87 prediction uncertainty of future water availability or water deficit is necessary (Taylor et al.,
88 2013). Kay and Davies (2008) compared the performance of the Penman-Monteith equation and
89 a simple temperature-based ET_0 method using climate data from five global and eight regional
90 climate models over Britain. They found that the two methods showed very different changes in
91 ET_0 for the period 2071-2100 under the A2 emission scenario, and different flow predictions for
92 three catchments when the data were used to force a rainfall-runoff model. Kay and Davies
93 results suggest that hydrological prediction uncertainty due to ET_0 formulation was smaller than
94 that due to GCM structure or RCM structure for their study region. Bae et al. (2011) evaluated
95 the uncertainty contributed by choice of GCM and hydrologic model for the Chungju Dam basin,
96 Korea. They found that hydrologic model structural differences contributed greater uncertainty
97 than GCM selection to winter runoff prediction. Koedyk and Kingston (2016) found that for the
98 Waikaia River, New Zealand ET_0 method contributed more uncertainty than GCM selection
99 when predicting ET_0 , but that runoff predictions were more sensitive to GCMs than to ET_0
100 methods. Thompson et al. (2014) evaluated the effect of using different GCMs and different ET_0
101 methods on discharge predictions for the Mekong River in Southeast Asia and found that GCM-
102 related uncertainty was greater than the ET_0 method related uncertainty.

103 In this study we perform a comprehensive evaluation of the relative sensitivity of future
104 P, ET_0 and water deficit (defined here as $P - ET_0$) projections to choice of GCM, ET_0 method and
105 RCP trajectory over the continental USA using CMIP5 GCM model outputs to provide new
106 insights that will inform more robust future water resource planning efforts. Variance-based
107 global sensitivity analysis (Saltelli et al., 2010) and Monte Carlo Filtering (Rose et al., 1991) are
108 used to quantify the uncertainty and important input factors controlling these projections. Global
109 sensitivity analysis (GSA) apportions the total output uncertainty simultaneously onto all the
110 uncertain input factors described by marginal probability density functions, and thus is preferred
111 over the local, one factor at a time, sensitivity analyses that have been previously reported
112 (Homma and Saltelli, 1996; Saltelli, 1999). Monte Carlo Filtering can identify sets of model
113 simulations and input factors that meet a specified criteria or threshold. Thus global sensitivity
114 analysis and Monte Carlo Filtering offer an opportunity to gain insight into the sources of
115 uncertainty, and drivers of particular types of wet/dry behavior, when estimating future water
116 deficit under projected climate change.

117

118 **2. Methods**

119 All retrospective and future climate variables were obtained from the CMIP5 archive
120 (accessible for download at <http://pcmdi9.llnl.gov/>). The “historical” runs of CMIP5 were used
121 for the retrospective period (1950-2005) and the same ensemble member runs (r1i1p1 ensemble)
122 of CMIP5 were used for two future periods: future period 1 (2030-2060), and future period 2
123 (2070-2100). Data for three RCP trajectories, RCP2.6, RCP4.5 and RCP8.5 were included in the
124 analyses. Taylor et al. (2012) described an overview of CMIP5 and RCP trajectories and
125 compared the differences between CMIP5 and CMIP3 model projections.

126 Data from the CMIP5 archive were used to calculate monthly mean P, ET_0 , and P- ET_0
127 (water deficit) for the retrospective and both future periods over each of the nine U.S. climate
128 regions identified by the National Climatic Data Center (Karl and Koss, 1984 (Fig. 1)). Future
129 changes in monthly mean P, ET_0 , and P- ET_0 were estimated by subtracting the monthly mean
130 value for the retrospective period from the monthly mean value for future period 1 or future
131 period 2, as appropriate (Baker and Huang, 2014).

132 Ten commonly used reference evapotranspiration estimation methods (Hargreaves,
133 Blaney-Criddle, Hamon, Kharrufa, Irmak-Rn, Irmak-Rs, Dalton, Meyer, Penman-Monteith and
134 Priestley-Taylor) were used in this study. The methods can be further classified into temperature-
135 (Hargreaves, Blaney-Criddle, Hamon and Kharrufa), radiation (Irmak-Rn, Irmak-Rs and
136 Priestley-Taylor), mass transfer (Dalton and Meyer), and combination (Penman-Monteith)
137 equations. These equations are well-described in many papers (e.g., Allen et al., 1998;
138 Hargreaves and Allen, 2003; Irmak et al., 2003; Tabari, 2010; Tabari et al., 2013; Xu and Singh,
139 2001) and are summarized in Table 1 (hereafter precipitation is referred to as P, and reference
140 evapotranspiration is referred to as ET_0 for convenience).

141 Variables directly used from the CMIP5 monthly model output included precipitation (pr,
142 P in this study), maximum and minimum temperature (tasmax and tasmin), radiation (rlds, rlus,
143 rsds, and rsus), air pressure (psl and ps), and wind speed (sfcWind). The abbreviations for these
144 variables are as defined in the CMIP5 archive and explained in the PCMDI server (Program For
145 Climate Model Diagnosis and Intercomparison, <http://cmip->

146 pcmdi.llnl.gov/cmip5/docs/standard_output.pdf). Other variables needed in the ten reference
 147 evapotranspiration equations were calculated using the variables from CMIP5 monthly model
 148 output (for details see Table 1). Monthly output that included all the variables needed for the
 149 Penman-Monteith reference evapotranspiration method (the most data intensive method) was
 150 available for both the retrospective period, and for the RCP2.6, RCP 4.5, and RCP8.5 trajectories
 151 for the future periods, for 9 CMIP5 models. Table 2 lists the 9 models from the CMIP5 archive
 152 that were used in this study.

153 The sensitivity of changes in future P, ET₀ and water deficit (defined here as P- ET₀) to
 154 the choice of GCM, ET₀ estimation method, and RCP trajectory was evaluated using the
 155 variance-based GSA method of Saltelli et al. (2010). Given a model of the form $Y =$
 156 $f(X_1, X_2, \dots, X_k)$, with Y a scalar, the variance-based first order effect for a generic factor X_i can
 157 be written (Saltelli et al., 2010):

$$158 \quad V_{X_i} \left(E_{X_{\sim i}}(Y|X_i) \right) \quad (1)$$

159 where X_i is the i -th factor (in our case either GCM, ET₀ method or RCP trajectory) and $X_{\sim i}$ is the
 160 vector of all factors except X_i . The expectation operator $E_{X_{\sim i}}(Y|X_i)$ indicates that the mean of
 161 Y is taken over all possible values of X except X_i (i.e. $X_{\sim i}$) while keeping X_i fixed. The variance,
 162 V_{X_i} , is then taken of this quantity over all possible values of X_i .

163 The first order sensitivity coefficient is expressed as:

$$164 \quad S_i = \frac{V_{X_i}(E_{X_{\sim i}}(Y|X))}{V(Y)} \quad (2)$$

165 Where $V(Y)$ the total variance of Y over all X_i . S_i is a normalized index varying between 0 and
 166 1, because $V_{X_i} \left(E_{X_{\sim i}}(Y|X_i) \right)$ varies between 0 and $V(Y)$ according to the identity (Mood et al.,
 167 1974):

$$168 \quad V_{X_i} \left(E_{X_{\sim i}}(Y|X_i) \right) + E_{X_i} \left(V_{X_{\sim i}}(Y|X_i) \right) = V(Y) \quad (3)$$

169 As indicated above $V_{X_i}(E_{X_{\sim i}}(Y|X_i))$ is the first order effect of X_i on the model output
 170 Y , while $E_{X_i}(V_{X_{\sim i}}(Y|X_i))$ is called the residual. The total effect index, including first order and
 171 higher order effects (i.e. interactions between factor X_i and other factors) of the factor X_i on the
 172 model output is calculated (Saltelli et al., 2010):

$$173 S_{T_i} = \frac{E_{X_{\sim i}}(V_{X_i}(Y|X_{\sim i}))}{V(Y)} = 1 - \frac{V_{X_{\sim i}}(E_{X_i}(Y|X_{\sim i}))}{V(Y)} \quad (4)$$

174 The first order sensitivity of estimated future changes in mean monthly P, ET₀, and P-
 175 ET₀ to choice of GCM, ET₀ estimation method and RCP trajectory were calculated over the nine
 176 US climate regions for each future period in order to evaluate the relative contributions of each
 177 of these factors on the uncertainty of future changes. A total of 270 simulations (9 GCMs × 10
 178 evapotranspiration methods × 3 RCP trajectories) was used in the analysis. Sensitivity of
 179 projected changes in P were evaluated for both choice of GCM and choice of RCP trajectory.
 180 Sensitivity of projected changes in ET₀ and P- ET₀ were evaluated for choice of GCM, choice of
 181 ET₀ estimation method, and choice of RCP trajectory.

182 For projected changes in water deficit (P- ET₀) Monte Carlo filtering (Saltelli et al., 2008)
 183 was used to identify whether projected wetter or drier future conditions (i.e. larger or smaller
 184 water deficit) could be attributed to specific GCMs, ET₀ estimation methods, or RCP trajectories.
 185 For each future period the ensemble of 270 projections of change in water deficit were
 186 categorized as either wet future condition (mean change in $(P - ET_0) \geq 0$) or dry future
 187 condition (mean change in $(P - ET_0) < 0$). Next for each factor (X_i =GCM, ET₀ method, RCP
 188 trajectory) the histograms of wet ($f_{wet}|X_i$) and dry ($f_{dry}|X_i$) future conditions over the range of
 189 possible values of that factor were estimated. To identify the factors that are most responsible for
 190 driving the model into projected wet or dry future conditions for each factor, X_i , the distributions
 191 ($f_{wet}|X_i$) and ($f_{dry}|X_i$) were tested for significant difference using the χ^2 two sample test for
 192 categorical variables with $\alpha=0.05$ (Rao and Scott, 1981). If for a given factor X_i the two
 193 distributions are significantly different, then X_i is a key factor in driving into either a wet or dry
 194 condition (Saltelli et al., 2008).

195 Because GCM predictions are known to contain systematic biases (Hwang and Graham,
196 2013; Wood et al., 2002, 2004) we evaluated the sensitivity of the mean monthly change in raw
197 climate predictions between retrospective and future periods to the choice of GCM, ET_0
198 estimation method and RCP trajectories. This is analogous to using the delta change GCM bias
199 correction method that involves shifting the mean of a series of observed climate data by the
200 mean difference in raw GCM output between the corresponding observed time period and the
201 desired future period. Teutschbein and Seibert (2012) pointed out that all bias correction methods
202 are based on the stationarity principle that assumes that similar biases occur in the retrospective
203 and future predictions and thus the same bias-correction algorithm may be applied to both.
204 Muerth et al. (2013) found that the impact of bias correction on the relative change of flow
205 indicators between retrospective and future periods was weak for most indicators, however
206 Pierce et al. (2015) found that some bias correction methods altered model-projected changes in
207 mean precipitation and temperature. LaFond et al. (2014) found that the delta change GCM bias
208 correction method was more useful for simulating hydrologic extreme events than the quantile
209 mapping bias correction method as it preserved daily climate variability better. In this study, we
210 differenced raw rather than bias corrected GCM outputs in order to prevent spurious alteration of
211 the climate change signal between retrospective and future GCMs that might be induced by the
212 bias correction method.

213

214 **3. Results**

215 3.1. Projected P, ET_0 , and water deficit change in the 21st century

216 Future P, ET_0 and water deficit projections include large uncertainties stemming from
217 different sources. Figures 2 and 3 present maps of the mean change (Fig. 2) and the standard
218 deviation of change (Fig. 3) in annual P (top chart), ET_0 (middle) and water deficit ($P - ET_0$;
219 bottom) over the continental US calculated over all GCMs, ET_0 estimation methods, and RCP
220 trajectories for future period 2 (2070-2100). Major portions of the West, Southwest and South
221 show a mean decrease in annual precipitation, while the rest of the continental US shows a mean
222 increase (Fig. 2 (a)). Future annual ET_0 shows a mean increase over retrospective annual ET_0
223 over the entire US (Fig. 2 (b)), with the largest increase in the South region. Following the

224 patterns of P and ET_0 , future annual water deficit ($P - ET_0$) shows a significant mean decrease in
225 the West, Southwest and South regions and a slight decline, or negligible change in most other
226 regions (Fig. 2 (c)). These mean changes in annual P, ET_0 and $P - ET_0$ are relatively small
227 compared to the standard deviation of changes in annual P, ET_0 , and $P - ET_0$ (Fig. 3). Water
228 deficit in particular has a large standard deviation, resulting in coefficients of variation larger
229 than one throughout the continental US. Similar results are shown in the Fig. S-1 and Fig. S-2 for
230 future period 1 (2030-2060) in the supplemental materials.

231 Figure 4 shows the seasonal changes in the monthly mean and standard deviation of
232 water deficit ($P - ET_0$) over the nine US regions. Blue and red lines represent the changes in
233 monthly mean water deficit for future period 1 and future period 2, respectively and the error
234 bars represent one standard deviation around each mean value. All regions of the continental US
235 show drier conditions (negative mean changes) in the summer season (Jun – Aug). Southern
236 regions (Southeast, South, Southwest and West) show drier conditions throughout the year,
237 however northern portions of the US (i.e. the Northeast, Ohio Valley, Upper Midwest, Northern
238 Rockies and Plains and Northwest) show wetter conditions (positive mean changes) in the winter
239 season.

240 3.2. Global sensitivity analysis of projected changes

241 Figure 5 shows the first order sensitivity of change in P to GCM and RCP trajectory over
242 the nine US climate regions for future periods 1 and 2. For projected changes in P, the choice of
243 GCM is generally more important than choice of RCP trajectory for all regions and both future
244 periods. First order sensitivities of mean change in ET_0 to GCM, ET_0 method and RCP
245 trajectory are shown in Fig. 6. This figure clearly shows that the choice of ET_0 method is the
246 most influential factor for projecting change in ET_0 for both future periods, except for the month
247 of March in the Northeast, Upper Midwest and Northern Rockies and Plains. High sensitivity of
248 mean change in ET_0 to GCM selection occurs in spring for several regions (Northeast, Upper
249 Midwest and Northern Rockies and Plains), indicating a divergence of model predictions during
250 this time. The influence of the RCP trajectory on ET_0 increases in future period 2 over future
251 period 1, with a concomitant decrease in the influence of both ET_0 method and GCM. In future
252 period 1 the GCM sensitivity coefficients are greater than the RCP trajectory sensitivity
253 coefficients over most regions; however, in future period 2 the RCP sensitivity coefficients

254 become more important. Figure 7 shows that projected change in water deficit depend strongly
255 on both the choice of GCM and ET_0 estimation method. In all regions except the Southeast
256 projected change in water deficit is most sensitive to ET_0 estimation method in the warm season
257 (May through October) and most sensitive to GCM in the cool season (December through
258 March). For the Southeast region the sensitivity coefficients for GCM and ET_0 method are quite
259 similar throughout the year. The sensitivity coefficients for RCP trajectory are very low in future
260 1, but increase in future 2, becoming approximately equal to the GCM sensitivity coefficients in
261 the summer season in future 2.

262 3.3. Change in annual mean water deficit projections using different ET_0 methods

263 Figure 8 shows the change in annual mean water deficit over all 9 GCMs for the RCP 4.5
264 trajectory in future period 1 (2030-2060) predicted by the ten different ET_0 methods used in this
265 study (a: Hargreaves, b: Blaney-Criddle, c: Hamon, d: Kharrufa, e: Irmak-Rn, f: Irmak-Rs, g:
266 Dalton, h: Meyer, i: Penman-Monteith, j: Priestley-Taylor). This figure clearly shows that the
267 changes in water deficit for future period 1 are diverse and depend strongly on the choice of ET_0
268 method. Except for the Hargreaves method (Fig. 8a) the temperature based methods (e.g.
269 Blaney-Criddle (Fig. 8b), Hamon (Fig. 8c) and Kharrufa (Fig. 8d)) predict drier conditions over
270 the continental US than the other methods. The mass transfer based methods (e.g Dalton (Fig.
271 8g) and Meyer (Fig. 8h)) predict generally wetter conditions over most of the continental US
272 compared to other methods. The combination method (Penman Monteith (Fig. 8i)), and the
273 radiation based methods (Irmak-Rn (Fig 8e), Irmak-Rs (Fig. 8f) and Priestley Taylor (Fig. 8j))
274 generally fall between the mass transfer based and temperature based methods, with the
275 combination methods producing slightly drier conditions. Although most methods predict similar
276 spatial patterns of water deficit over the continental US (generally drier conditions in the West,
277 Southwest and South and generally wetter elsewhere), the Hamon method predicts a different
278 pattern of water deficit over the Southwest, South and Northern Rockies and Plains regions.

279 3.4. Monte Carlo filtering

280 Monte Carlo filtering (Saltelli et al., 2008) was conducted to further investigate whether
281 projected wetter or drier future conditions (i.e. larger or smaller annual mean water deficit) could
282 be attributed to specific GCMs, ET_0 estimation methods, or RCP trajectories. Figures 9 shows

283 the histograms for wet conditions and dry conditions in future 2 over the Southeast US by GCM,
284 ET₀ method and RCP trajectory for the example month of July. Figure 10 shows similar
285 histograms for the Northern Rockies and Plains, a region with differing behavior from the
286 Southeast US. Table 3 shows the P-value results for the X^2 - test for all months in both futures for
287 the Southeast and Northern Rockies and Plains regions. P-values greater than 0.05 (shaded in
288 grey) indicate the two histograms are not significantly different from each other. Tables 4 – 6
289 show the fraction of time that a particular GCM (Table 4), ET₀ method (Table 5), or RCP
290 trajectory (Table 6) projected drier future conditions in each of the nine US climate regions for
291 each month, with fractions higher than 0.5 shaded in grey.

292

293 **4. Discussion**

294 Drier conditions in southern regions (Southeast, South, Southwest and West) and wetter
295 conditions in northern regions (Northeast, Ohio Valley, Upper Midwest, Northern Rockies and
296 Plains and Northwest) are consistent (Fig. 4) with those reported by McAfee (2013) who used 3
297 ET₀ methods (Hamon, Priestley-Taylor and Penman-Monteith) to estimate global changes in ET₀
298 over the entire globe. As found by Baker and Huang (2014) for both CMIP3 and CMIP5
299 projections, mean ET₀ is projected to be higher in future period 2 than in future period 1, and
300 mean precipitation projections are approximately equivalent in future period 1 and future period
301 2. Thus the projected mean changes in water deficit for future period 2 (red lines in Fig. 4) are
302 larger in magnitude than the projected changes for future period 1 (blue lines). In all regions, and
303 for both future periods, the one standard deviation error bars bracket zero mean change
304 indicating large uncertainty in the projections throughout the year.

305 The choice of GCM is generally more important than the choice of RCP trajectory for
306 projected changes in P (Fig. 5). This is consistent with results found by Gaetani and Mohino
307 (2013) and Knutti and Sedláček (2012) who showed significant differences in precipitation
308 predictions among CMIP5 models. It should be noted that these results do not indicate that the
309 choice of RCP trajectory does not affect the change in precipitation, only that the choice of RCP
310 trajectory is less influential than the choice of GCM. There are no consistent seasonal patterns of
311 the first-order sensitivity coefficients for either GCM or RCP trajectory in either future period.

312 However, during the spring months, the sensitivity of change in P to choice of RCP trajectory
313 increases substantially in future 2 compared to future 1 in the Northeast, Ohio Valley, Upper
314 Midwest, South, Southwest and West regions.

315 Higher sensitivity of mean change in ET_0 to the choice of ET_0 estimation method than the
316 choice of GCM (Fig. 6) are consistent with those found by Kingston et al. (2009) who showed
317 that projected increase in ET_0 varied by more than 100% between ET_0 methods, and Schwalm et
318 al. (2013) who found the choice of ET_0 estimation method is sensitive and even more influential
319 than the choice of GCM in predicting ET_0 . However, neither of these studies looked at the
320 influence of RCP trajectory on ET_0 projections, which increases in future period 2 over future
321 period 1, causing a decrease in the sensitivity coefficient of both GCM and ET_0 method in future
322 2. Burke and Brown (2008) evaluated uncertainties in the projection of future drought using
323 several drought indices. They found that there are large uncertainties in regional changes in
324 drought and changes in drought are dependent on both index definition and GCM ensemble
325 members. Similarly, our results for the projected change in water deficit vary by region, depend
326 strongly on the choice of GCM and ET_0 estimation method, but are relatively less sensitive to
327 RCP trajectory (Fig. 7). These findings are similar to results reported by Orłowski and
328 Seneviratne (2013) who found that the greenhouse gas emission scenario uncertainty is not as
329 important as differences among GCMs or internal climate variability when predicting
330 Standardized Precipitation Index (SPI) and soil moisture (SMA). However, they also found that
331 uncertainty due to greenhouse gas emission scenario increased in later future periods. Taylor et
332 al. (2013) showed the patterns of changes in future drought were similar between the A1B
333 scenario in CMIP3 and the RCP2.6 trajectory in CMIP5, reinforcing our finding that the choice
334 of RCP trajectory is less important than the choice of GCM and ET_0 estimation method when
335 estimating future water deficit.

336 Similar to the results of Kay and Davies (2008) and Bae et al. (2011) the results of our
337 GSA show that the choice of ET_0 method has important implications when making future ET_0
338 projections and future water deficit projections (Fig. 8). Kingston et al. (2009) recommended the
339 use of different ET_0 equations to evaluate global ET_0 , and Wang et al. (2015) found that although
340 different methods predict similar future ET_0 , there are important differences in uncertainties due
341 to ET_0 estimation methods and input data reliability. Currently many hydrological models use a

342 single evapotranspiration method for simulation, which may substantially increase the
343 uncertainty and reduce the reliability of future projections. Our results strongly indicate that an
344 ensemble of ET_0 estimation methods should be used to understand potential future water
345 availability and water deficit due to climate change.

346 Monte Carlo filtering results (Fig. 9 and 10, Table 3) indicate that GCM and ET_0 methods
347 both produce statistically significant different wet condition and dry condition histograms in both
348 the Southeast and Northern Rockies and Plains regions for almost all months in both future
349 periods. This indicates that particular GCMs and ET_0 methods tend to systematically produce
350 wet or dry conditions. Some GCMs (i.e. MIROC_ESM and BCC-CSM (Table 4)) and ET_0
351 methods (i.e. Priestley-Taylor, Blaney-Criddle, and Kharrufa (Table 5)) predict dry conditions a
352 majority of the time for all regions in both future periods. However, the remaining GCMs and
353 ET_0 methods project both wetter or drier futures depending on the region and future period.
354 Results in Tables 4 through 6 show that for the South, West and Southwest regions drier
355 conditions are predicted a majority of the time in both future periods by all GCMs and RCP
356 trajectories, and all ET_0 methods except Hargreaves. For RCP trajectory, P-values indicate the
357 histograms are statistically significantly different in fewer cases than for either GCM or ET_0
358 method for both future 1 and 2 (Table 3). These results are consistent with the first order
359 sensitivity coefficients results that showed the RCP trajectory is not as important a factor as
360 GCM or ET_0 method in driving differences in future projections, but that the sensitivity to choice
361 of RCP trajectory increases in future period 2.

362 GCMs estimate some climate variables, such as temperature, with higher confidence than
363 other variables (Randall et al., 2007). However, for some evapotranspiration estimation methods
364 the effect of temperature on evaporation is smaller than other climate variables (Linacre, 1994;
365 Roderick et al., 2009a, 2009b; Thom et al., 1981). We found that temperature and net radiation
366 from the CMIP5 GCMs show increasing trends over the 2005-2100 time period, while wind
367 speed and surface pressure are relatively constant (Fig. S-3). Because we considered various ET_0
368 estimation methods our results include the impacts of the different physics represented in the ET_0
369 methods, the projected changes each of the climate variables contributing to the different ET_0
370 methods, and the reliability of the predictions of each variable.

371

372 **5. Summary and Conclusions**

373 Future changes in precipitation and evapotranspiration will lead to changes in the
374 hydrologic balance. This study clearly shows that the uncertainty caused by different GCMs, ET₀
375 methods, and RCP trajectories make actionable water resources planning based on climate
376 change projections difficult. Understanding and quantifying how these projected changes vary
377 with choice of GCM, ET₀ method and RCP trajectory is important for designing robust
378 ensembles of scenarios to include in future water resources planning. This study assessed the
379 future mean change in monthly precipitation, evapotranspiration and water deficit (P- ET₀)
380 projected by CMIP5 simulations over the continental US and analyzed the sensitivity of the
381 projected changes to the choice of GCM, ET₀ estimation method, and RCP trajectory. Nine
382 GCMs, ten ET₀ estimation methods, and three RCP trajectories were included in the analyses.
383 Variance-based global sensitivity analysis (Saltelli et al., 2010) was conducted in order to
384 determine the relative contributions of the choice of GCMs, ET₀ estimation methods, and RCP
385 trajectory to uncertainty in future prediction. Monte Carlo filtering was used to investigate
386 whether particular GCMs, ET₀ methods, and/or RCP scenarios consistently led to wet or dry
387 future projections.

388 The global sensitivity analyses showed that projected changes in precipitation are more
389 sensitive to the choice of GCM than the choice of RCP trajectory over the entire continental US
390 for both future periods. However, the choice of RCP trajectory becomes more important in future
391 period 2. The most sensitive factor for the future ET₀ projections is the choice of ET₀ estimation
392 method for all regions in both future periods. The first order sensitivity of projected change in
393 future ET₀ to choice of RCP trajectory increases in future period 2 compared to future 1, with a
394 concomitant decrease in the first order sensitivity to the choice of GCM. For projected change in
395 future water deficit the choice of ET₀ method constitutes the dominant source of uncertainty in
396 warmer months (May through September) and the choice of GCM is the dominant source of
397 uncertainty in the cooler months (November through March) over all regions except the
398 Southeast where the sensitivity of GCM and ET₀ method are roughly equal throughout the year.
399 Sensitivity of change in future water deficit to RCP trajectory is very small for future period 1,
400 but increased in future period 2.

401 Monte Carlo filtering results indicated that both GCMs and ET_0 methods produced
402 statistically different histograms for wetter or drier future conditions (i.e. larger or smaller mean
403 future water deficit) for almost all months in both future periods. Two GCMs (MIROC_ESM
404 and BCC-CSM) and three ET_0 methods (Priestley-Taylor, Blaney-Criddle, and Kharrufa)
405 predicted dry conditions a majority of the time for all regions in both future periods; however,
406 the remaining GCMs and ET_0 methods projected both wetter and drier futures depending on the
407 region.

408 Results of this study indicate that when predicting the effects of future climate on water
409 resources the choice of evapotranspiration method should be carefully evaluated. Rather than the
410 typical practice of using a single ET_0 method to drive a hydrologic model with future climate
411 projections, an ensemble of ET_0 methods should be used in addition to an ensemble of GCMs
412 and a variety of RCP trajectories. The GSA methodology adopted here assumed that all the
413 GCMs, ET_0 methods and RCP trajectories used in this study were equally appropriate for use in
414 all US regions (i.e. the sensitivity coefficients were evaluated by equally weighting each GCMs,
415 ET_0 method and RCP trajectory) which is likely not to be the case. When making future
416 projections potential climate change on water resources Reliability Ensemble Averaging (REA)
417 (Giorgi and Mearns, 2002) or Bayesian-based indicator-weighting (Asefa and Adams, 2013;
418 Tebaldi et al., 2005; Xing et al., 2014) could be used to weight the results of an ensemble of
419 GCMs and ET methods based on how close the retrospective GCM- ET_0 method predictions
420 agree with past observations (bias criterion) and how well the future GCM- ET_0 -RCP
421 projections agree with other future GCM- ET_0 -RCP predictions (convergence criterion).

422 This study assumed that ET_0 methods that have been developed and parameterized based
423 on vegetation response to current CO_2 levels and climatic conditions will be valid under future
424 CO_2 levels and climatic conditions. Future research should explore the validity of this
425 assumption by incorporating potential changes in plant transpiration (e.g. stomatal conductance)
426 to changing CO_2 levels into the ET_0 estimation methodologies.

427

428 **Acknowledgements**

429 This research was supported by Tampa Bay Water and the University of Florida Water
430 Institute. We acknowledge the modeling groups participating in the Program for Climate Model
431 Diagnosis and Inter-comparison (PCMDI) for their role in making the CMIP5 (Coupled Model
432 Intercomparison Project) multi-model data set available.

433 **References**

- 434 Allen, R. G., Pereira, L. S., Raes, D. and Smith, M.: Crop evapotranspiration: guidelines for
435 computing crop water requirements. FAO Irrigation and Drainage Paper 56., 1998.
- 436 Asefa, T. and Adams, A.: Reducing bias-corrected precipitation projection uncertainties: a
437 Bayesian-based indicator-weighting approach, *Reg. Environ. Chang.*, 13(S1), 111–120,
438 doi:10.1007/s10113-013-0431-9, 2013.
- 439 Baker, N. C. and Huang, H.-P.: A Comparative Study of Precipitation and Evaporation between
440 CMIP3 and CMIP5 Climate Model Ensembles in Semiarid Regions, *J. Clim.*, 27(10), 3731–
441 3749, doi:10.1175/JCLI-D-13-00398.1, 2014.
- 442 Bentsen, M., Bethke, I., Debernard, J. B., Iversen, T., Kirkevåg, A., Seland, Ø., Drange, H.,
443 Roelandt, C., Seierstad, I. A., Hoose, C. and Kristjánsson, J. E.: The Norwegian Earth System
444 Model, NorESM1-M – Part 1: Description and basic evaluation of the physical climate, *Geosci.
445 Model Dev.*, 6(3), 687–720, doi:10.5194/gmd-6-687-2013, 2013.
- 446 Block, K. and Mauritsen, T.: Forcing and feedback in the MPI-ESM-LR coupled model under
447 abruptly quadrupled CO₂, *J. Adv. Model. Earth Syst.*, 5(4), 676–691, doi:10.1002/jame.20041,
448 2013.
- 449 Burke, E. J. and Brown, S. J.: Evaluating Uncertainties in the Projection of Future Drought, *J.
450 Hydrometeorol.*, 9(2), 292–299, doi:10.1175/2007JHM929.1, 2008.
- 451 Chaouche, K., Neppel, L., Dieulin, C., Pujol, N., Ladouche, B., Martin, E., Salas, D. and
452 Caballero, Y.: Analyses of precipitation, temperature and evapotranspiration in a French
453 Mediterranean region in the context of climate change, *Comptes Rendus Geosci.*, 342(3), 234–
454 243, doi:10.1016/j.crte.2010.02.001, 2010.
- 455 Chong-Hai, X. and Ying, X.: The projection of temperature and precipitation over China under
456 RCP scenarios using a CMIP5 multi-model ensemble, *Atmos. Ocean. Sci. Lett.*, 5(6), 527–533,
457 doi:10.1080/16742834.2012.11447042, 2012.
- 458 Gaetani, M. and Mohino, E.: Decadal prediction of the sahelian precipitation in CMIP5
459 simulations, *J. Clim.*, 26(19), 7708–7719, doi:10.1175/JCLI-D-12-00635.1, 2013.
- 460 Georgakakos, A., Fleming, P., Dettinger, M., Peters-Lidard, C., Richmond, T., Reckhow, K.,
461 White, K. and Yates, D.: Ch. 3: Water Resources. *Climate Change Impacts in the United States:
462 The Third National Climate Assessment.*, 2014.
- 463 Giorgi, F. and Mearns, L.: Calculation of average, uncertainty range, and reliability of regional
464 climate changes from AOGCM simulations via the “reliability ensemble averaging”(REA)
465 method, *J. Clim.*, 15(10), 1141–1158, doi:http://dx.doi.org/10.1175/1520-
466 0442(2002)015<1141:COAURA>2.0.CO;2, 2002.
- 467 Guo, H., Golaz, J.-C., Donner, L. J., Ginoux, P. and Hemler, R. S.: Multivariate Probability
468 Density Functions with Dynamics in the GFDL Atmospheric General Circulation Model: Global
469 Tests, *J. Clim.*, 27(5), 2087–2108, doi:10.1175/JCLI-D-13-00347.1, 2014.
- 470 Hargreaves, G. H. and Allen, R. G.: History and Evaluation of Hargreaves Evapotranspiration
471 Equation, *J. Irrig. Drain. Eng.*, 129(1), 53–63, doi:10.1061/(ASCE)0733-9437(2003)129:1(53),
472 2003.
- 473 Hawkins, E. and Sutton, R.: The potential to narrow uncertainty in regional climate predictions,

474 Bull. Am. Meteorol. Soc., 90(8), 1095–1107, doi:10.1175/2009BAMS2607.1, 2009.

475 Hawkins, E. and Sutton, R.: The potential to narrow uncertainty in projections of regional
476 precipitation change, *Clim. Dyn.*, 37(1-2), 407–418, doi:10.1007/s00382-010-0810-6, 2010.

477 Homma, T. and Saltelli, A.: Importance measures in global sensitivity analysis of nonlinear
478 models, *Reliab. Eng. Syst. Saf.*, 52(1), 1–17, doi:10.1016/0951-8320(96)00002-6, 1996.

479 Hwang, S. and Graham, W. D.: Development and comparative evaluation of a stochastic analog
480 method to downscale daily GCM precipitation, *Hydrol. Earth Syst. Sci.*, 17(11), 4481–4502,
481 doi:10.5194/hess-17-4481-2013, 2013.

482 Irmak, S., Irmak, A., Allen, R. G. and Jones, J. W.: Solar and Net Radiation-Based Equations to
483 Estimate Reference Evapotranspiration in Humid Climates, *J. Irrig. Drain. Eng.*, 129(5), 336–
484 347, doi:10.1061/(ASCE)0733-9437(2003)129:5(336), 2003.

485 Ishak, A. M., Bray, M., Remesan, R. and Han, D.: Estimating reference evapotranspiration using
486 numerical weather modelling, *Hydrol. Process.*, 24(24), 3490–3509, doi:10.1002/hyp.7770,
487 2010.

488 Ji, D., Wang, L., Feng, J., Wu, Q., Cheng, H., Zhang, Q., Yang, J., Dong, W., Dai, Y., Gong, D.,
489 Zhang, R.-H., Wang, X., Liu, J., Moore, J. C., Chen, D. and Zhou, M.: Description and basic
490 evaluation of BNU-ESM version 1, *Geosci. Model Dev. Discuss.*, 7(2), 1601–1647,
491 doi:10.5194/gmdd-7-1601-2014, 2014.

492 Johnson, F. and Sharma, A.: Measurement of GCM Skill in Predicting Variables Relevant for
493 Hydroclimatological Assessments, *J. Clim.*, 22(16), 4373–4382, doi:10.1175/2009JCLI2681.1,
494 2009.

495 Karl, T. R. and Koss, W. J.: Historical Climatology Series 4-3: Regional and National Monthly,
496 Seasonal, and Annual Temperature Weighted by Area, 1895-1983., 1984.

497 Kharin, V. V., Zwiers, F. W., Zhang, X. and Wehner, M.: Changes in temperature and
498 precipitation extremes in the CMIP5 ensemble, *Clim. Change*, 119(2), 345–357,
499 doi:10.1007/s10584-013-0705-8, 2013.

500 Kingston, D. G., Todd, M. C., Taylor, R. G., Thompson, J. R. and Arnell, N. W.: Uncertainty in
501 the estimation of potential evapotranspiration under climate change, *Geophys. Res. Lett.*, 36(20),
502 L20403, doi:10.1029/2009GL040267, 2009.

503 Knutti, R. and Sedláček, J.: Robustness and uncertainties in the new CMIP5 climate model
504 projections, *Nat. Clim. Chang.*, 3(4), 369–373, doi:10.1038/nclimate1716, 2012.

505 LaFond, K. M., Griffis, V. W. and Spellman, P.: Forcing Hydrologic Models with GCM Output:
506 Bias Correction vs. the “Delta Change” Method, in *World Environmental and Water Resources*
507 *Congress 2014*, vol. 1, pp. 2146–2155, American Society of Civil Engineers, Reston, VA., 2014.

508 Linacre, E. T.: Estimating U.S. Class A Pan Evaporation from Few Climate Data, *Water Int.*,
509 19(1), 5–14, doi:10.1080/02508069408686189, 1994.

510 Maurer, E. P. and Hidalgo, H. G.: Utility of daily vs. monthly large-scale climate data: an
511 intercomparison of two statistical downscaling methods, *Hydrol. Earth Syst. Sci.*, 12(2), 551–
512 563, doi:10.5194/hess-12-551-2008, 2008.

513 McAfee, S. A.: Methodological differences in projected potential evapotranspiration, *Clim.*
514 *Change*, 120(4), 915–930, doi:10.1007/s10584-013-0864-7, 2013.

515 Mood, A. M., Graybill, F. A. and Boes, D. C.: Introduction to theory of statistics, McGraw-Hill,
516 Inc., 1974.

517 Orłowsky, B. and Seneviratne, S. I.: Elusive drought: uncertainty in observed trends and short-
518 and long-term CMIP5 projections, *Hydrol. Earth Syst. Sci.*, 17(5), 1765–1781, doi:10.5194/hess-
519 17-1765-2013, 2013.

520 Quintana Seguí, P., Ribes, A., Martin, E., Habets, F. and Boé, J.: Comparison of three
521 downscaling methods in simulating the impact of climate change on the hydrology of
522 Mediterranean basins, *J. Hydrol.*, 383(1-2), 111–124, doi:10.1016/j.jhydrol.2009.09.050, 2010.

523 Randall, D. A., Wood, R. A., Bony, S., Colman, R., Fichet, T., Fyfe, J., Kattsov, V., Pitman,
524 A., Shukla, J., Srinivasan, J., Stouffer, R. J., Sumi, A. and Taylor, K. E.: Climate Models and
525 Their Evaluation, in *Climate Change 2007: The Physical Science Basis. Contribution of Working
526 Group I to the Fourth Assessment Report of the Intergovernmental Panel on Climate Change*,
527 edited by S. Solomon, D. Qin, M. Manning, Z. Chen, M. Marquis, K. B. Averyt, M. Tignor, and
528 H. L. Miller, pp. 591–662, Cambridge University Press, Cambridge, United Kingdom and New
529 York, NY, USA., 2007.

530 Rao, J. N. K. and Scott, A. J.: The Analysis of Categorical Data From Complex Sample Survey :
531 Chi-Squared Tests for Goodness of Fit and Independence in Two-Way Tables, *J. Am. Stat.*
532 *Assoc.*, 76(374), 221–230, 1981.

533 Roderick, M. L., Hobbins, M. T. and Farquhar, G. D.: Pan Evaporation Trends and the
534 Terrestrial Water Balance. I. Principles and Observations, *Geogr. Compass*, 3(2), 746–760,
535 doi:10.1111/j.1749-8198.2008.00213.x, 2009a.

536 Roderick, M. L., Hobbins, M. T. and Farquhar, G. D.: Pan Evaporation Trends and the
537 Terrestrial Water Balance. II. Energy Balance and Interpretation, *Geogr. Compass*, 3(2), 761–
538 780, doi:10.1111/j.1749-8198.2008.00214.x, 2009b.

539 Rose, K. A., Smith, E. P., Gardner, R. H., Brenkert, A. L. and Bartell, S. M.: Parameter
540 sensitivities, monte carlo filtering, and model forecasting under uncertainty, *J. Forecast.*,
541 10(October 1989), 117–133, doi:10.1002/for.3980100108, 1991.

542 Rotstayn, L. D., Jeffrey, S. J., Collier, M. A., Dravitzki, S. M., Hirst, A. C., Syktus, J. I. and
543 Wong, K. K.: Aerosol- and greenhouse gas-induced changes in summer rainfall and circulation
544 in the Australasian region: a study using single-forcing climate simulations, *Atmos. Chem.*
545 *Phys.*, 12(14), 6377–6404, doi:10.5194/acp-12-6377-2012, 2012.

546 Saltelli, A.: Sensitivity analysis: Could better methods be used?, *J. Geophys. Res.*, 104(D3),
547 3789, doi:10.1029/1998JD100042, 1999.

548 Saltelli, A., Annoni, P., Azzini, I., Campolongo, F., Ratto, M. and Tarantola, S.: Variance based
549 sensitivity analysis of model output. Design and estimator for the total sensitivity index, *Comput.*
550 *Phys. Commun.*, 181(2), 259–270, doi:10.1016/j.cpc.2009.09.018, 2010.

551 Saltelli, A., Ratto, M., Andres, T., Campolongo, F., Cariboni, J., Gatelli, D., Saisana, M. and
552 Tarantola, S.: *Global sensitivity analysis: the primer*, John Wiley & Sons, Inc., 2008.

553 Schwalm, C. R., Huntzger, D. N., Michalak, A. M., Fisher, J. B., Kimball, J. S., Mueller, B.,
554 Zhang, K. and Zhang, Y.: Sensitivity of inferred climate model skill to evaluation decisions: a
555 case study using CMIP5 evapotranspiration, *Environ. Res. Lett.*, 8(2), 024028,
556 doi:10.1088/1748-9326/8/2/024028, 2013.

557 Sung, J. H., Kang, H.-S., Park, S., Cho, C., Bae, D. H. and Kim, Y.-O.: Projection of Extreme
558 Precipitation at the end of 21st Century over South Korea based on Representative Concentration
559 Pathways (RCP), *Atmosphere (Basel)*, 22(2), 221–231, doi:10.14191/Atmos.2012.22.2.221,
560 2012.

561 Tabari, H.: Evaluation of Reference Crop Evapotranspiration Equations in Various Climates,
562 *Water Resour. Manag.*, 24(10), 2311–2337, doi:10.1007/s11269-009-9553-8, 2010.

563 Tabari, H., Grismer, M. E. and Trajkovic, S.: Comparative analysis of 31 reference
564 evapotranspiration methods under humid conditions, *Irrig. Sci.*, 31(2), 107–117,
565 doi:10.1007/s00271-011-0295-z, 2013.

566 Taylor, I. H., Burke, E., McColl, L., Falloon, P. D., Harris, G. R. and McNeall, D.: The impact of
567 climate mitigation on projections of future drought, *Hydrol. Earth Syst. Sci.*, 17(6), 2339–2358,
568 doi:10.5194/hess-17-2339-2013, 2013.

569 Taylor, K. E., Stouffer, R. J. and Meehl, G. A.: An Overview of CMIP5 and the Experiment
570 Design, *Bull. Am. Meteorol. Soc.*, 93(4), 485–498, doi:10.1175/BAMS-D-11-00094.1, 2012.

571 Tebaldi, C., Smith, R. L., Nychka, D. and Mearns, L. O.: Quantifying Uncertainty in Projections
572 of Regional Climate Change: A Bayesian Approach to the Analysis of Multimodel Ensembles, *J.*
573 *Clim.*, 18(10), 1524–1540, doi:10.1175/JCLI3363.1, 2005.

574 Teutschbein, C. and Seibert, J.: Bias correction of regional climate model simulations for
575 hydrological climate-change impact studies: Review and evaluation of different methods, *J.*
576 *Hydrol.*, 456-457, 12–29, doi:10.1016/j.jhydrol.2012.05.052, 2012.

577 Thom, A. S., Thony, J.-L. and Vauclin, M.: On the proper employment of evaporation pans and
578 atmometers in estimating potential transpiration, *Q. J. R. Meteorol. Soc.*, 107(453), 711–736
579 [online] Available from: <http://dx.doi.org/10.1002/qj.49710745316>, 1981.

580 Thomas, A.: Spatial and temporal characteristics of potential evapotranspiration trends over
581 China, *Int. J. Climatol.*, 20(4), 381–396, doi:10.1002/(SICI)1097-
582 0088(20000330)20:4<381::AID-JOC477>3.0.CO;2-K, 2000.

583 Walsh, J., Wuebbles, D., Hayhoe, K., Kossin, J., Stephens, G., Thorne, P., Vose, R., Wehner, M.,
584 Willis, J., Anderson, D., Doney, S., Feely, R., Hennon, P., Kharin, V., Knutson, T., Landerer, F.,
585 Lenton, T., Kennedy, J. and Somerville, R.: Ch. 2: Our Changing Climate. *Climate Change*
586 *Impacts in the United States: The Third National Climate Assessment.*, 2014.

587 Wang, W., Xing, W. and Shao, Q.: How large are uncertainties in future projection of reference
588 evapotranspiration through different approaches?, *J. Hydrol.*, 524, 696–700,
589 doi:10.1016/j.jhydrol.2015.03.033, 2015.

590 Wang, W., Xing, W., Shao, Q., Yu, Z., Peng, S., Yang, T., Yong, B., Taylor, J. and Singh, V. P.:
591 Changes in reference evapotranspiration across the Tibetan Plateau: Observations and future
592 projections based on statistical downscaling, *J. Geophys. Res. Atmos.*, 118(10), 4049–4068,
593 doi:10.1002/jgrd.50393, 2013.

594 Watanabe, S., Hajima, T., Sudo, K., Nagashima, T., Takemura, T., Okajima, H., Nozawa, T.,
595 Kawase, H., Abe, M., Yokohata, T., Ise, T., Sato, H., Kato, E., Takata, K., Emori, S. and
596 Kawamiya, M.: MIROC-ESM: model description and basic results of CMIP5-20c3m
597 experiments, *Geosci. Model Dev. Discuss.*, 4(2), 1063–1128, doi:10.5194/gmdd-4-1063-2011,
598 2011.

599 Wood, A. W., Leung, L. R., Sridhar, V. and Lettenmaier, D. P.: Hydrologic implications of
600 dynamical and statistical approaches to downscaling climate model outputs, *Clim. Change*, 62(1-
601 3), 189–216, doi:10.1023/B:CLIM.0000013685.99609.9e, 2004.

602 Wood, A. W., Maurer, E. P., Kumar, A. and Lettenmaier, D. P.: Long-range experimental
603 hydrologic forecasting for the eastern United States, *J. Geophys. Res.*, 107(D20), 4429,
604 doi:10.1029/2001JD000659, 2002.

605 Xiao-Ge, X., Tong-Wen, W., Jiang-Long, L., Zai-Zhi, W., Wei-Ping, L. and Fang-Hua, W.: How
606 well does BCC_CSM1. 1 reproduce the 20th century climate change over China?, *Atmos.*
607 *Ocean. Sci. Lett.*, 6(1), 21–26 [online] Available from:
608 <http://159.226.119.58/aos/CN/article/downloadArticleFile.do?attachType=PDF&id=332>
609 (Accessed 12 January 2015), 2013.

610 Xing, W., Wang, W., Shao, Q., Peng, S., Yu, Z., Yong, B. and Taylor, J.: Changes of reference
611 evapotranspiration in the Haihe River Basin: Present observations and future projection from
612 climatic variables through multi-model ensemble, *Glob. Planet. Change*, 115, 1–15,
613 doi:10.1016/j.gloplacha.2014.01.004, 2014.

614 Xu, C., Gong, L., Jiang, T., Chen, D. and Singh, V. P.: Analysis of spatial distribution and
615 temporal trend of reference evapotranspiration and pan evaporation in Changjiang (Yangtze
616 River) catchment, *J. Hydrol.*, 327(1-2), 81–93, doi:10.1016/j.jhydrol.2005.11.029, 2006.

617 Xu, C. and Singh, V.: Cross comparison of empirical equations for calculating potential
618 evapotranspiration with data from Switzerland, *Water Resour. Manag.*, 16(3), 197–219,
619 doi:10.1023/A:1020282515975, 2002.

620 Xu, C. and Singh, V. P.: Evaluation and generalization of temperature-based methods for
621 calculating evaporation, *Hydrol. Process.*, 15(2), 305–319, doi:10.1002/hyp.119, 2001.

622 Yukimoto, S., Adachi, Y., Hosaka, M., Sakami, T., Yoshimura, H., Hirabara, M., Tanaka, T. Y.,
623 Shindo, E., Tsujino, H., Deushi, M., Mizuta, R., Yabu, S., Obata, A., Nakano, H., Koshiro, T.,
624 Ose, T. and Kitoh, A.: A New Global Climate Model of the Meteorological Research Institute:
625 MRI-CGCM3 -Model Description and Basic Performance-, *J. Meteorol. Soc. Japan*, 90A, 23–
626 64, doi:10.2151/jmsj.2012-A02, 2012.

627 Zhao, L., Xia, J., Xu, C., Wang, Z., Sobkowiak, L. and Long, C.: Evapotranspiration estimation
628 methods in hydrological models, *J. Geogr. Sci.*, 23(2), 359–369, doi:10.1007/s11442-013-1015-
629 9, 2013.

630

631

632 Table 1. Description of reference evapotranspiration estimation methods used in this study (ET₀:
633 Reference evapotranspiration).

Methods	Equations ¹	Reference
(a) Hargreaves	$ET_0 = 0.0135K_T S_0 (T + 17.8) \sqrt{\delta_T}$	Hargreaves and Allen (2003)
(b) Blaney-Criddle	$ET_0 = p(0.46T + 8.13)$	Xu and Singh (2002)
(c) Hamon	$ET_0 = 0.55\delta_T^2 P_t$	Xu and Singh (2002)
(d) Kharrufa	$ET_0 = 0.34pT^{1.3}$	Xu and Singh (2002)
(e) Irmak-Rn	$ET_0 = 0.486 + 0.289R_n + 0.023T$	Irmak et al. (2003)
(f) Irmak-Rs	$ET_0 = -0.611 + 0.149R_s + 0.079T$	Irmak et al. (2003)
(g) Dalton	$ET_0 = (0.3648 + 0.07223u)(e_s - e_a)$	Tabari et al. (2013)
(h) Meyer	$ET_0 = (0.375 + 0.05026u)(e_s - e_a)$	Tabari et al. (2013)
(i) Penman-Monteith	$ET_0 = \frac{0.408\Delta(R_n - G) + \gamma \frac{900}{T + 273} u_2 (e_s - e_a)}{\Delta + \gamma(1 + 0.34u_2)}$	Allen et al. (1998)
(j) Priestley-Taylor	$ET_0 = \alpha \frac{\Delta}{\Delta + \gamma} \frac{(R_n - G)}{\lambda}$	Allen et al. (1998)

634 ¹Variables (estimated from CMIP5 outputs): G: Soil heat flux (assumed 0); γ : Psychrometric constant; T: Average
635 temperature; u_2 : Wind speed at 2m surface; e_s : Saturated vapor pressure; e_a : Actual vapor pressure; Δ : Slope vapor
636 pressure; K_T : Hargreaves-Samani coefficient; S_0 : Extraterrestrial radiation (estimated by Julian date); δ_T : Difference
637 between maximum and minimum temperature, p: Percentage of total daytime hours (Estimated by Julian date); R_n :
638 Net radiation; R_s : Solar radiation; P_t : Saturated water vapor density; u: Wind speed

639 Table 2. Description of the CMIP5 models used in this study.

Model	Institute (country)	Resolutions	Calendar	Reference
(1) BNU-ESM	College of Global Change and Earth System Science, Beijing Normal University (China)	2.8° lat × 2.8° lon	No leap	Ji et al. (2014)
(2) CSIRO-MK3-6-0	University of New South Wales (Australia)	1.87° lat × 1.87° lon	No leap	Rotstayn et al. (2012)
(3) GFDL-CM3	NOAA/Geophysical Fluid Dynamics Laboratory (USA)	2.0° lat × 2.5° lon	No leap	Guo et al. (2014)
(4) GFDL-ESM2G	NOAA/Geophysical Fluid Dynamics Laboratory (USA)	2.0° lat × 2.5° lon	No leap	Taylor et al. (2012)
(5) MIROC-ESM	Atmosphere and Ocean Research Institute, National Institute for Environmental Studies, and Japan Agency for Marine-Earth Science and Technology (Japan)	2.8° lat × 2.8° lon	Leap year	Watanabe et al. (2011)
(6) MPI-ESM-LR	Max Planck Institute for Meteorology (Germany)	1.87° lat × 1.87° lon	Leap year	Block and Mauritsen (2013)
(7) MRI-CGCM3	Meteorological Research Institute (Japan)	1.12° lat × 1.12° lon	Leap year	Yukimoto et al. (2012)
(8) NorESM1-M	Norwegian Climate Centre (Norway)	1.9° lat × 2.5° lon	No leap	Bentsen et al. (2013)
(9) BCC-CSM1.1	Beijing Climate Center (China)	2.8° lat × 2.8° lon	No leap	Xiao-Ge et al. (2013)

640

641 Table 3. P-values of Chi-square two sample test for difference among wet condition versus dry
 642 condition pdfs Southeast U.S (SE US) and Northern Rockies and Plains (NRP; West North
 643 Central) U.S. (Shaded cells indicate pdfs are not statistically significantly different at p=0.05)

Month		Future 1			Future 2		
		GCM	ET ₀	RCP	GCM	ET ₀	RCP
SE US	1	0.0000	0.0689	0.3701	0.0000	0.1823	0.1853
	2	0.0000	0.0889	0.4434	0.0000	0.0269	0.0000
	3	0.0000	0.0365	0.0306	0.0000	0.0000	0.1339
	4	0.0000	0.0000	0.6602	0.0000	0.0000	0.0001
	5	0.0000	0.0000	0.3223	0.0000	0.0000	0.0041
	6	0.0000	0.0000	0.0809	0.0000	0.0000	0.0006
	7	0.0000	0.0000	0.2855	0.0000	0.0000	0.0749
	8	0.0000	0.0000	0.2805	0.0000	0.0000	0.0074
	9	0.0000	0.0000	0.8646	0.0000	0.0000	0.0044
	10	0.0000	0.0000	0.0000	0.0000	0.0000	0.0001
	11	0.0000	0.0001	0.0000	0.0000	0.0001	0.2003
	12	0.0000	0.0117	0.3083	0.0000	0.0000	0.0000
NRP	1	0.0000	0.0000	0.1931	0.0000	0.0000	0.0000
	2	0.0000	0.0000	0.0010	0.0000	0.0000	0.7617
	3	0.0000	0.0000	0.0538	0.0000	0.0000	0.0769
	4	0.0000	0.0000	0.7882	0.0002	0.0000	0.8925
	5	0.0000	0.0000	0.4047	0.0000	0.0000	0.1103
	6	0.0000	0.0000	0.3839	0.0000	0.0000	0.0000
	7	0.0000	0.0000	0.5321	0.0001	0.0008	0.0000
	8	0.0000	0.0001	0.1544	0.0000	0.0686	0.0000
	9	0.0000	0.0000	0.4242	0.0000	0.0000	0.2002
	10	0.0000	0.0000	0.6688	0.0000	0.0213	0.0001
	11	0.0000	0.0000	0.1334	0.0000	0.0000	0.1948
	12	0.0000	0.0000	0.7617	0.0000	0.0000	0.6561

644

645

646 Table 4. The fraction of future dry conditions over all months by GCM (Future period 1 and 2).

	GCM	SE	South	West	NR	NE	NW	UM	SW	Ohio
Future period 1 - Dry condition	BNU_ESM	0.575	0.589	0.511	0.367	0.436	0.322	0.467	0.453	0.492
	CSIRO_mk3_6_0	0.489	0.689	0.639	0.547	0.297	0.519	0.381	0.653	0.481
	GFDL_CM3	0.414	0.608	0.686	0.419	0.403	0.525	0.383	0.647	0.425
	GFDL_ESM2G	0.731	0.900	0.758	0.453	0.486	0.486	0.397	0.828	0.617
	MIROC_ESM	0.631	0.594	0.822	0.625	0.636	0.708	0.686	0.658	0.611
	MPI_ESM_LR	0.375	0.747	0.694	0.542	0.597	0.611	0.558	0.756	0.575
	MRI_CGCM3	0.494	0.592	0.639	0.400	0.544	0.553	0.350	0.547	0.506
	NorESM1_M	0.492	0.764	0.778	0.475	0.400	0.611	0.475	0.753	0.508
	BCC_CSM	0.728	0.739	0.828	0.642	0.603	0.614	0.564	0.822	0.656
Future period 2 - Dry condition	BNU_ESM	0.608	0.775	0.597	0.400	0.522	0.461	0.478	0.522	0.572
	CSIRO_mk3_6_0	0.367	0.667	0.583	0.528	0.225	0.528	0.433	0.633	0.461
	GFDL_CM3	0.467	0.767	0.789	0.461	0.514	0.542	0.508	0.794	0.469
	GFDL_ESM2G	0.722	0.831	0.694	0.478	0.519	0.525	0.397	0.672	0.581
	MIROC_ESM	0.672	0.686	0.897	0.742	0.731	0.728	0.700	0.739	0.664
	MPI_ESM_LR	0.442	0.800	0.778	0.519	0.542	0.639	0.450	0.800	0.450
	MRI_CGCM3	0.508	0.703	0.581	0.422	0.481	0.528	0.439	0.517	0.556
	NorESM1_M	0.594	0.808	0.722	0.500	0.461	0.550	0.481	0.731	0.594
	BCC_CSM	0.628	0.697	0.875	0.708	0.567	0.708	0.556	0.825	0.603

647

648

649 Table 5. The fraction of future dry condition over all months by ET₀ estimation method and
 650 region (Future period 1 and 2).

	ET ₀	SE	South	West	NR	NE	NW	UM	SW	Ohio
Future period 1 -Dry condition	Hargreaves	0.302	0.426	0.559	0.333	0.309	0.466	0.321	0.485	0.324
	Blaney_Criddle	0.738	0.880	0.898	0.840	0.738	0.762	0.784	0.904	0.769
	Hamon	0.633	0.818	0.667	0.531	0.494	0.497	0.457	0.713	0.549
	Kharrufa	0.883	0.957	0.889	0.636	0.667	0.698	0.636	0.886	0.738
	Irmak_Rn	0.522	0.673	0.694	0.491	0.512	0.556	0.494	0.679	0.580
	Irmak_Rs	0.525	0.722	0.731	0.463	0.485	0.546	0.460	0.679	0.556
	Dalton	0.364	0.503	0.583	0.340	0.343	0.426	0.296	0.509	0.380
	Meyer	0.367	0.531	0.596	0.346	0.324	0.435	0.290	0.512	0.367
	PM	0.534	0.685	0.694	0.472	0.469	0.525	0.481	0.676	0.540
	PT	0.608	0.719	0.750	0.515	0.552	0.590	0.515	0.753	0.608
Future period 2 -Dry condition	Hargreaves	0.352	0.506	0.605	0.420	0.355	0.491	0.380	0.537	0.361
	Blaney_Criddle	0.765	0.907	0.880	0.877	0.769	0.818	0.830	0.901	0.806
	Hamon	0.633	0.861	0.679	0.552	0.491	0.528	0.460	0.719	0.574
	Kharrufa	0.883	0.954	0.898	0.704	0.713	0.728	0.682	0.883	0.784
	Irmak_Rn	0.515	0.738	0.710	0.494	0.491	0.574	0.503	0.685	0.543
	Irmak_Rs	0.534	0.796	0.753	0.485	0.497	0.562	0.478	0.719	0.562
	Dalton	0.349	0.596	0.620	0.389	0.358	0.475	0.315	0.540	0.373
	Meyer	0.352	0.596	0.630	0.383	0.349	0.488	0.309	0.546	0.361
	PM	0.543	0.744	0.701	0.475	0.485	0.531	0.463	0.679	0.528
	PT	0.639	0.784	0.765	0.509	0.562	0.593	0.515	0.716	0.608

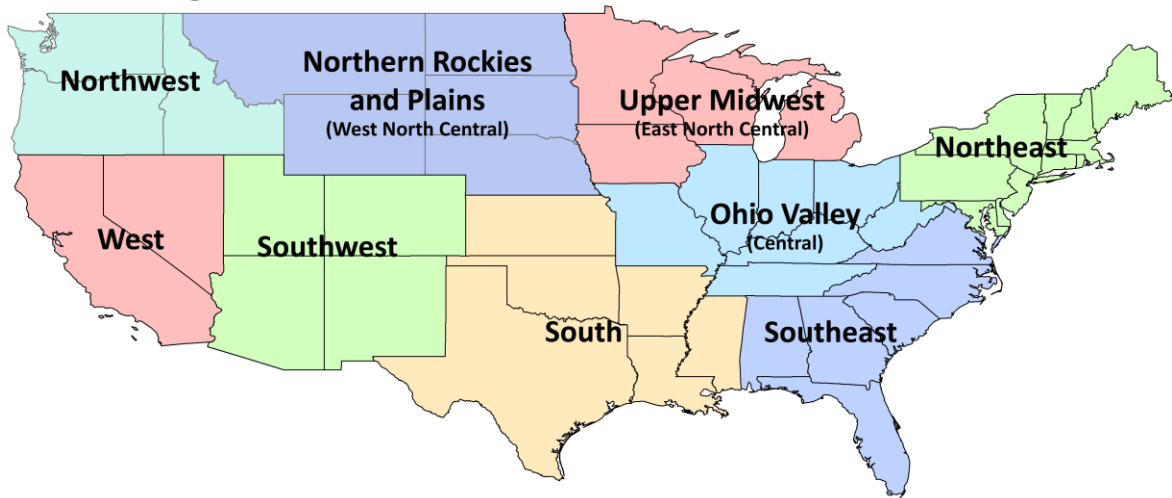
651

652 Table 6. The fraction of future dry condition over all months by RCP trajectory and region
 653 (Future period 1 and 2).

	RCP	SE	South	West	NR	NE	NW	UM	SW	Ohio
Future period 1 -Dry condition	2.6	0.551	0.657	0.665	0.507	0.502	0.543	0.495	0.644	0.553
	4.5	0.553	0.698	0.739	0.515	0.475	0.554	0.482	0.731	0.556
	8.5	0.539	0.719	0.715	0.468	0.491	0.554	0.443	0.665	0.515
Future period 2 -Dry condition	2.6	0.516	0.649	0.657	0.486	0.524	0.515	0.465	0.617	0.545
	4.5	0.490	0.731	0.712	0.510	0.476	0.584	0.494	0.658	0.528
	8.5	0.664	0.864	0.803	0.590	0.520	0.637	0.521	0.803	0.577

654

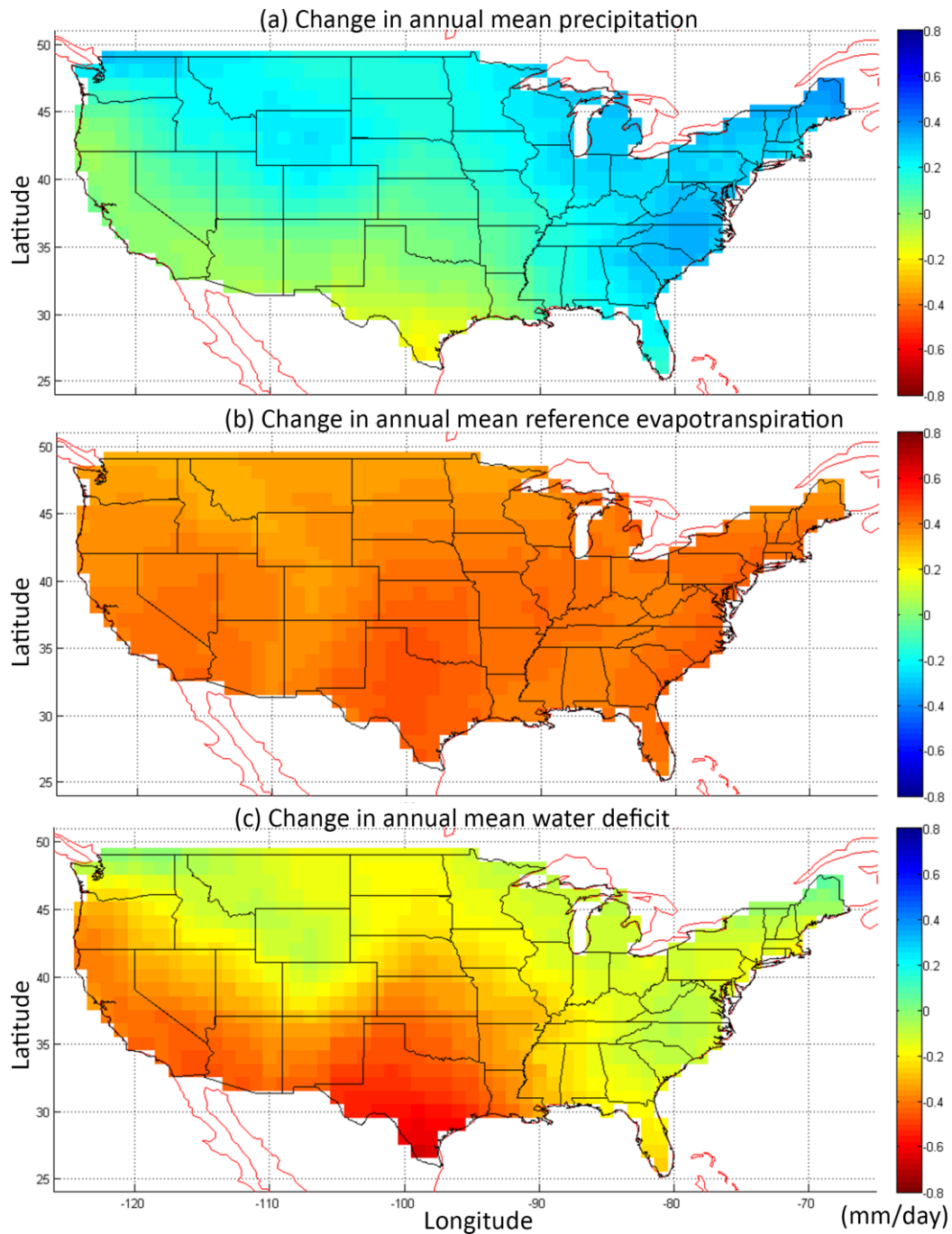
US Climate Regions



655

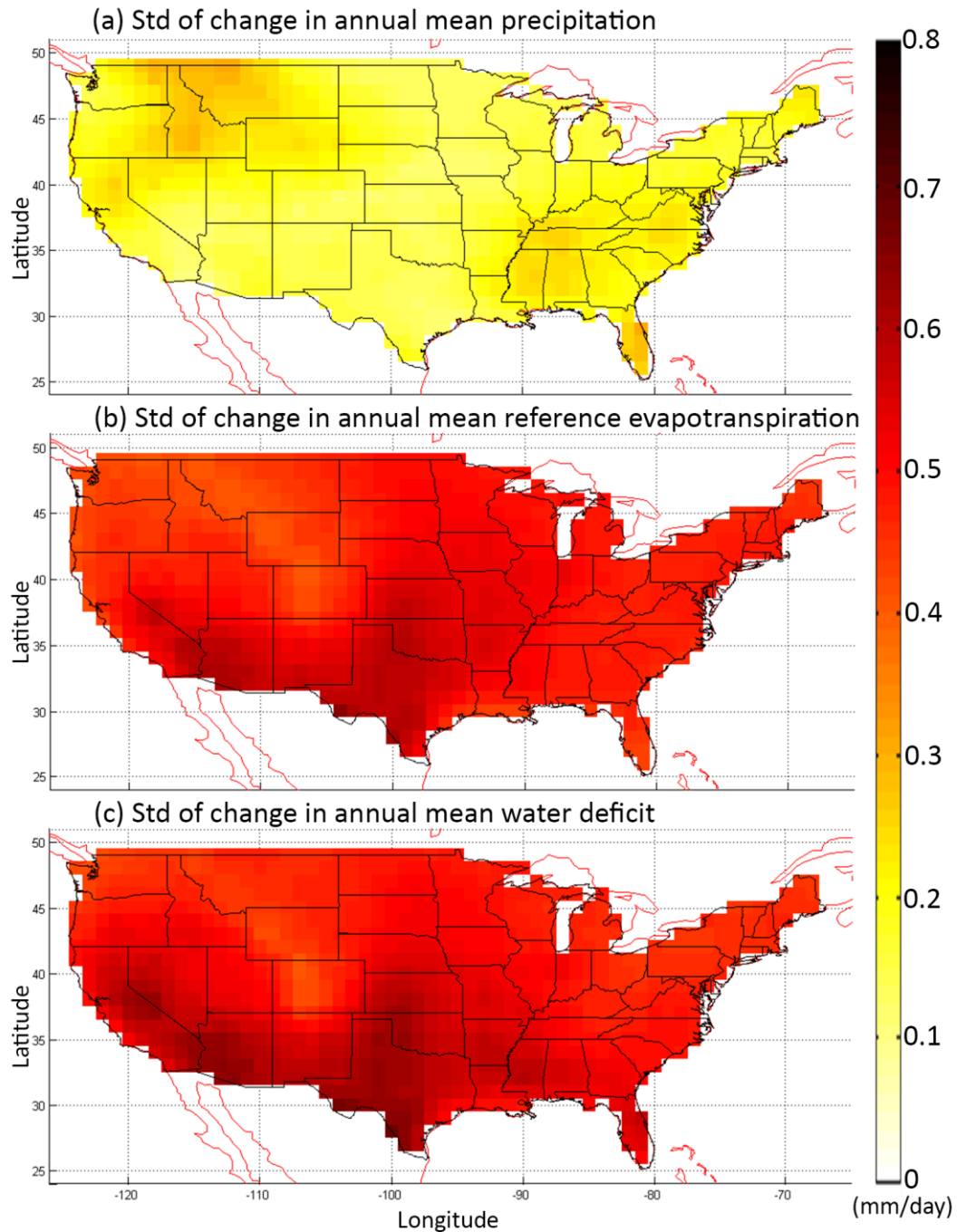
656 Figure 1. US climate regions identified by National Climate Data Center (Adapted from Karl and

657 Koss, 1984, <https://www.ncdc.noaa.gov/monitoring-references/maps/us-climate-regions.php>)



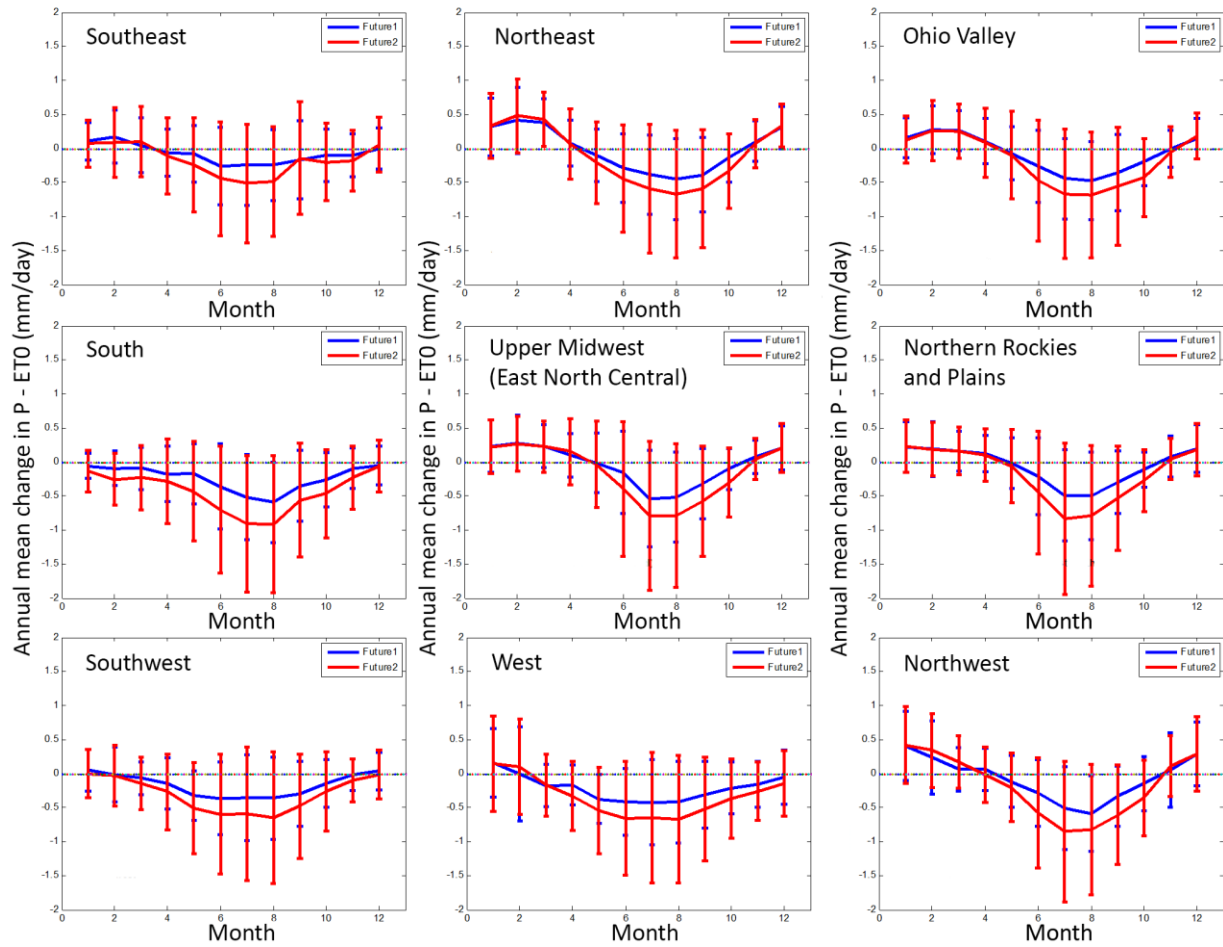
658

659 Figure 2. The change in the annual mean (a) P, (b) ET_0 , and (c) $P - ET_0$ over U.S. All units are
 660 mm/day and the change is defined as the mean of 2070-2100 minus that of 1950-2005. These
 661 changes are averaged over all GCMs, ET_0 estimation methods, and RCP trajectories.



662

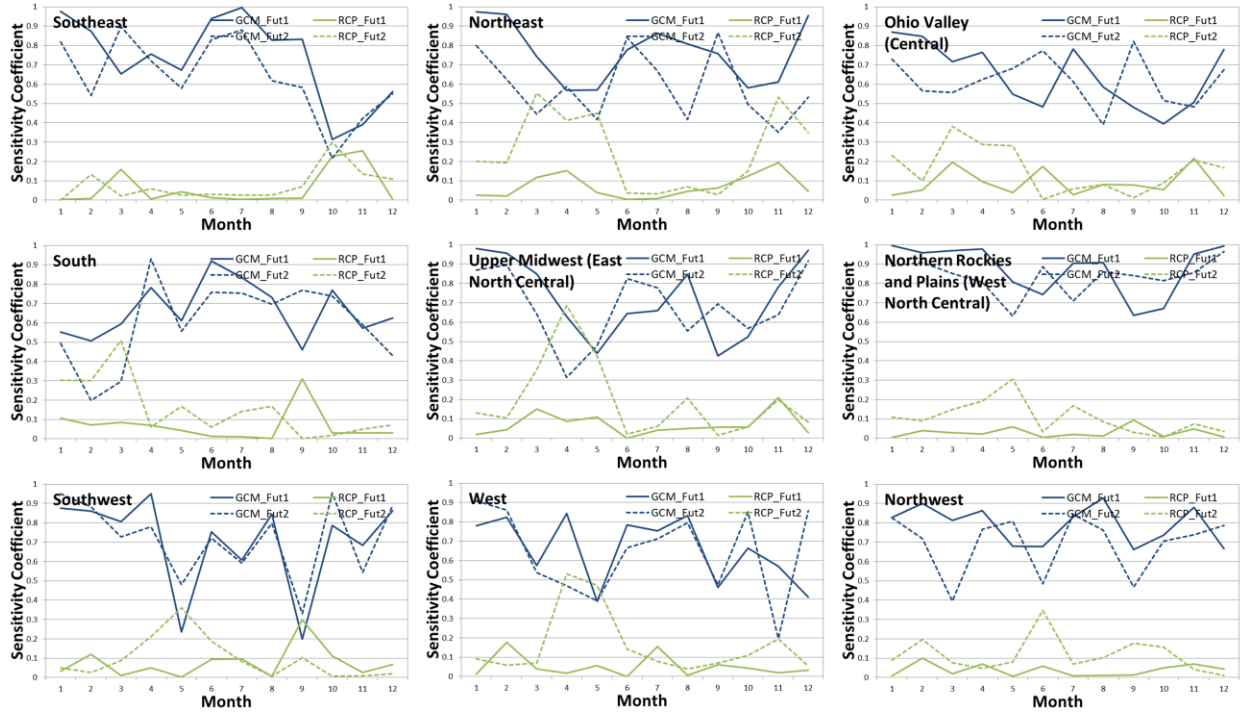
663 Figure 3. The standard deviation of the change in the annual mean (a) P, (b) ET_0 , and (c) $P - ET_0$
 664 over U.S. All units are mm/day and the change is defined as the average of 2070-2100 minus that
 665 of 1950-2005. The standard deviations are estimated over all GCMs, ET_0 estimation methods,
 666 and RCP trajectories.



667

668 Figure 4. The change of monthly mean water deficit ($P - ET_0$) over 9 different regions. Blue
 669 lines represent future 1 period (2030-2060), and red lines represent future 2 period (2070-2100).
 670 Error bars represent one standard deviation of each values. The change is defined as the mean of
 671 future periods minus that of retrospective period (1950-2005).

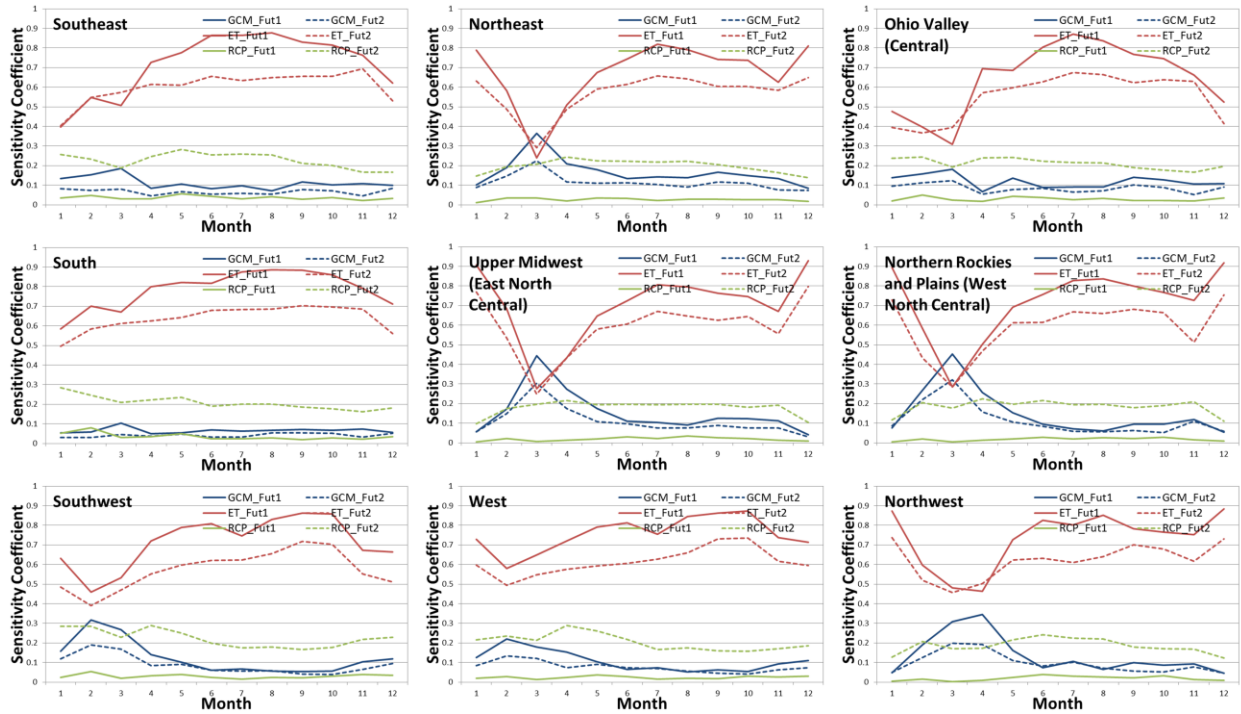
672



673

674 Figure 5. First order sensitivity analysis results of change in precipitation. Solid lines represent
 675 the future period 1 (2030-2060) and dotted lines represent the future period 2 (2070-2100). Blue
 676 lines represent the first order effect of GCMs and green lines represent the first order effect of
 677 RCPs.

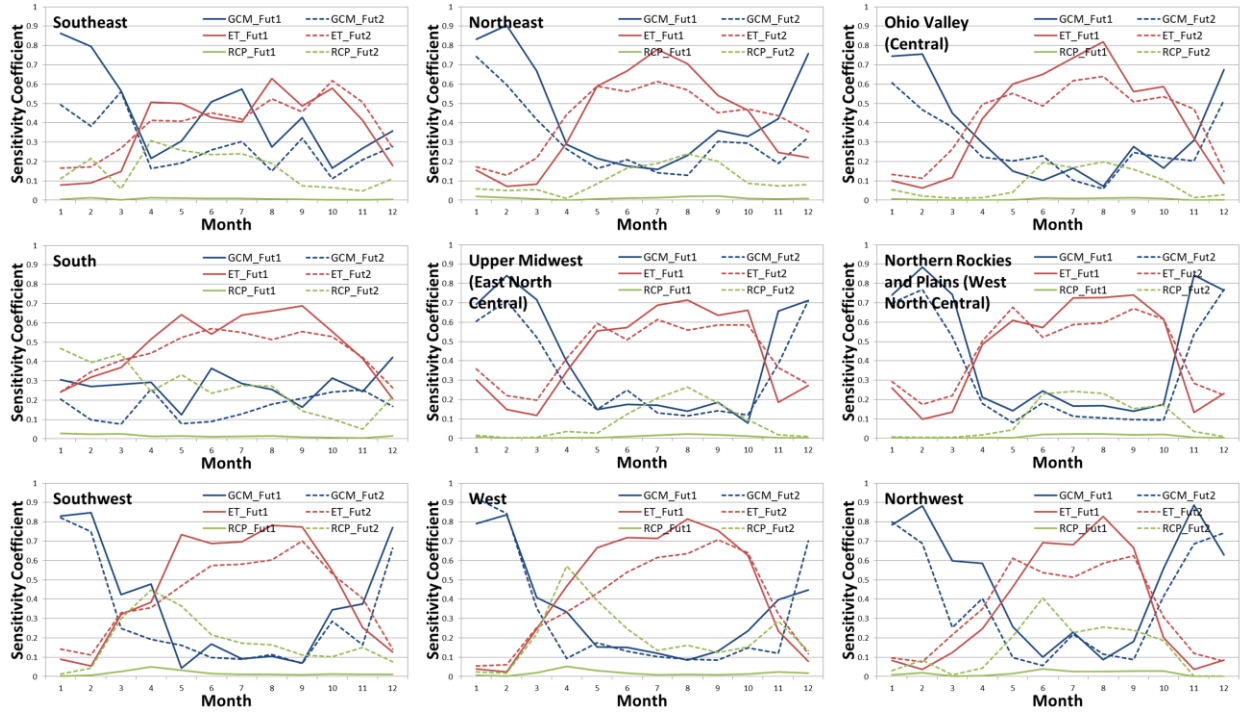
678



679

680 Figure 6. First order sensitivity analysis results of change in reference evapotranspiration. Solid
 681 lines represent the future period 1 (2030-2060) and dotted lines represent the future period 2
 682 (2070-2100). Blue lines represent the first order effect of GCMs, red lines represent the first
 683 order effect of ET_0 estimation methods and green lines represent the first order effect of RCPs.

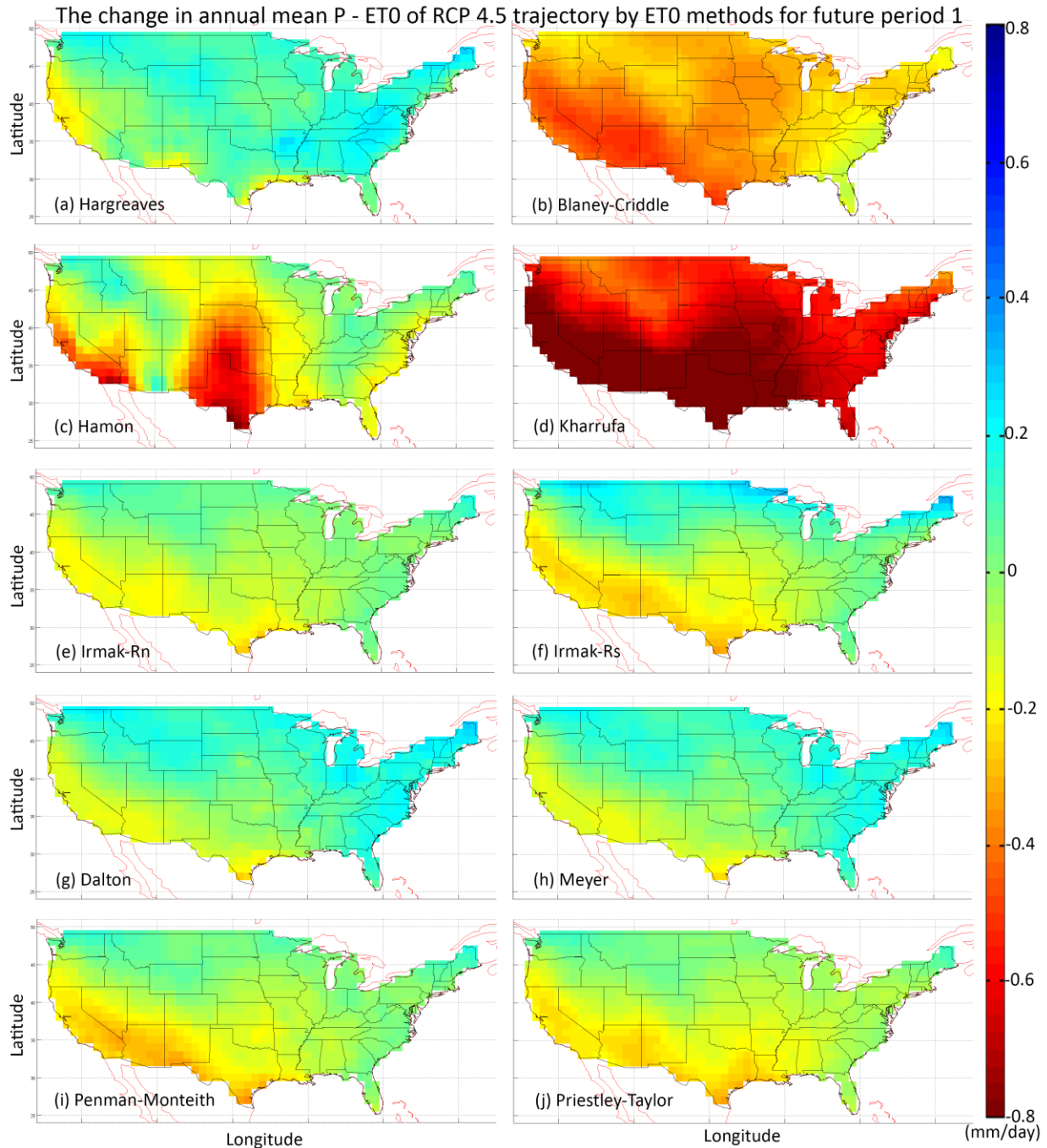
684



685

686 Figure 7. First order sensitivity analysis results of change in $P - ET_0$. Solid lines represent the
 687 future period 1 (2030-2060) and dotted lines represent the future period 2 (2070-2100). Blue
 688 lines represent the first order effect of GCMs, red lines represent the first order effect of ET_0
 689 estimation methods and green lines represent the first order effect of RCPs.

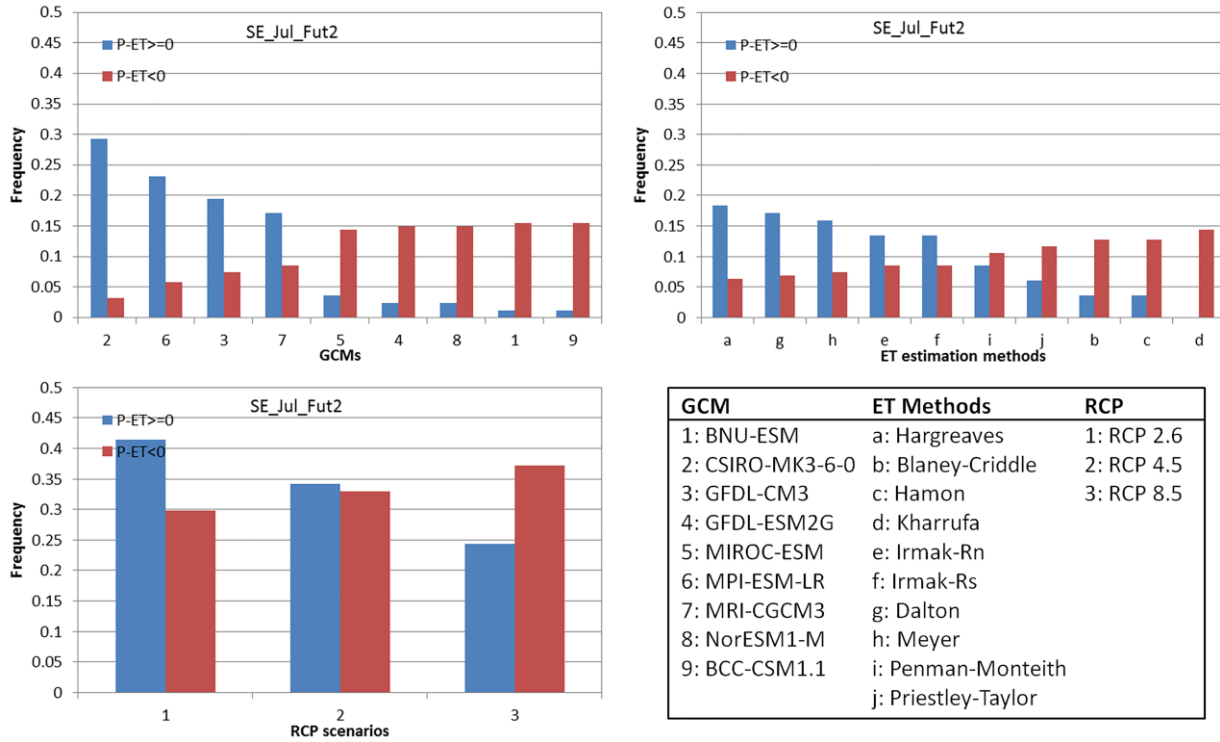
690



691

692 Figure 8. The change in the annual mean P – ET₀ of RCP 4.5 scenario by 10 different
 693 evapotranspiration methods. All units are mm/day and the change is defined as the mean of
 694 2030-2060 minus that of 1950-2005. (All results are interpolated to 1 degree * 1 degree grids and
 695 averaged over 9 different GCMs)

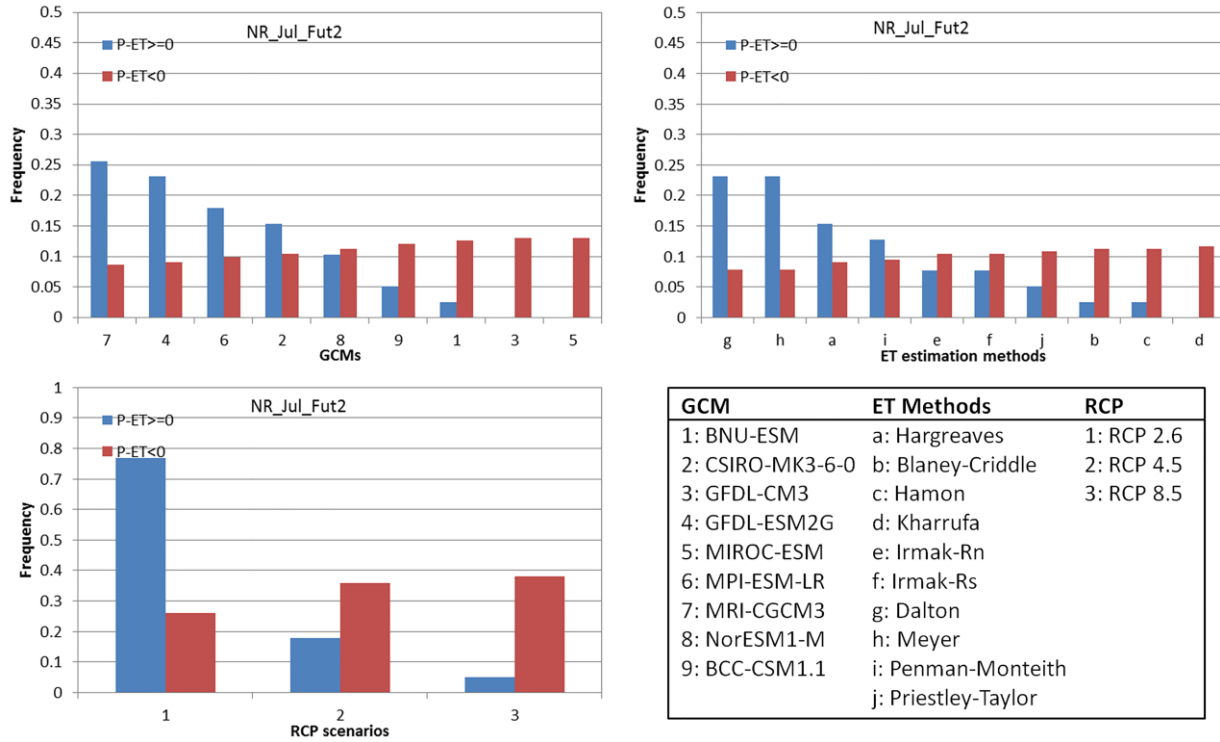
696



697

698 Figure 9. Histograms for projected future 2 wet conditions and dry conditions in the Southeast
 699 US by GCM, ET_0 method and RCP trajectory for the month of July.

700

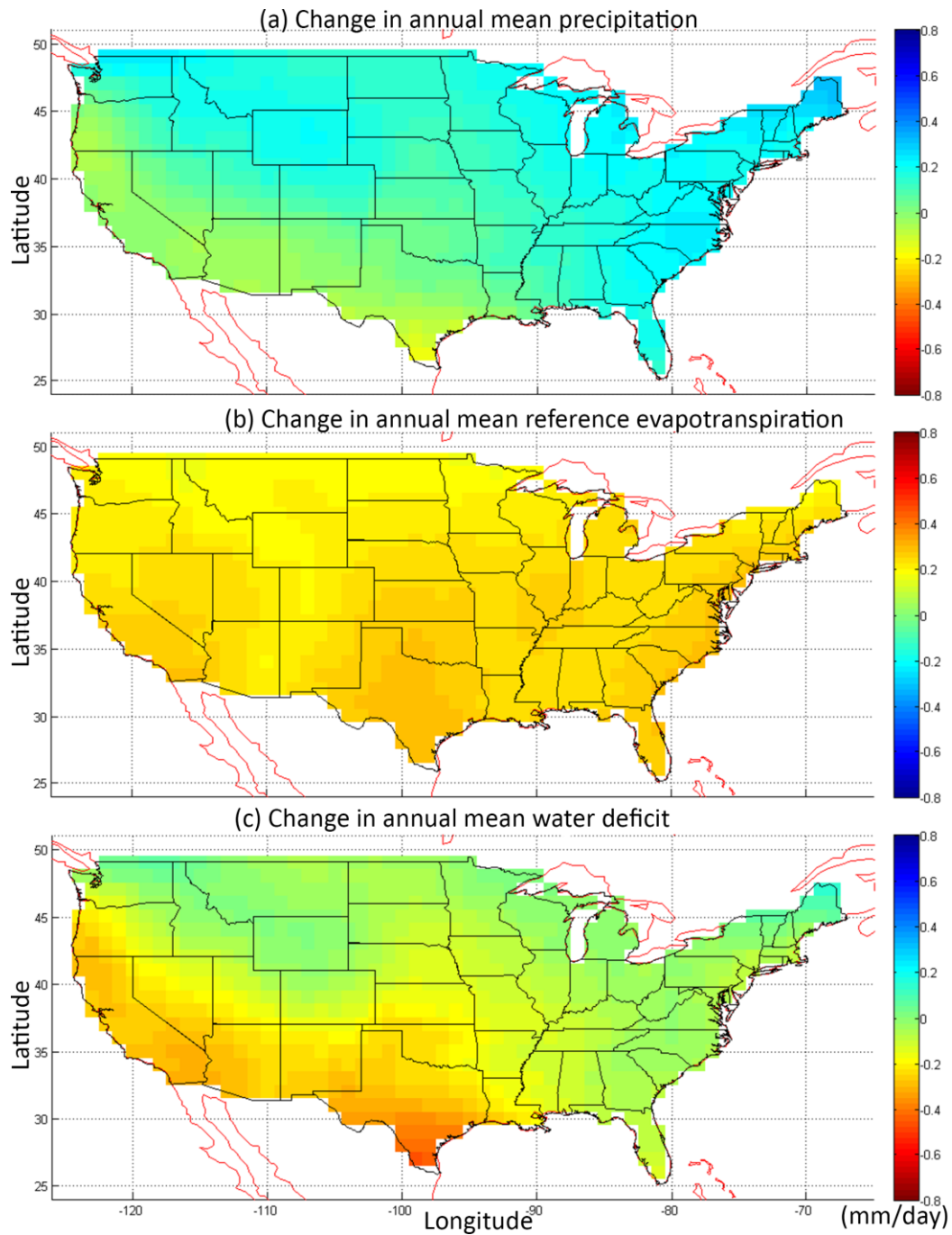


701

702 Figure 10. Histograms for projected future 2 wet conditions and dry conditions in the Northern
 703 Rockies and Plains US by GCM, ET₀ method and RCP trajectory for the month of July.

704

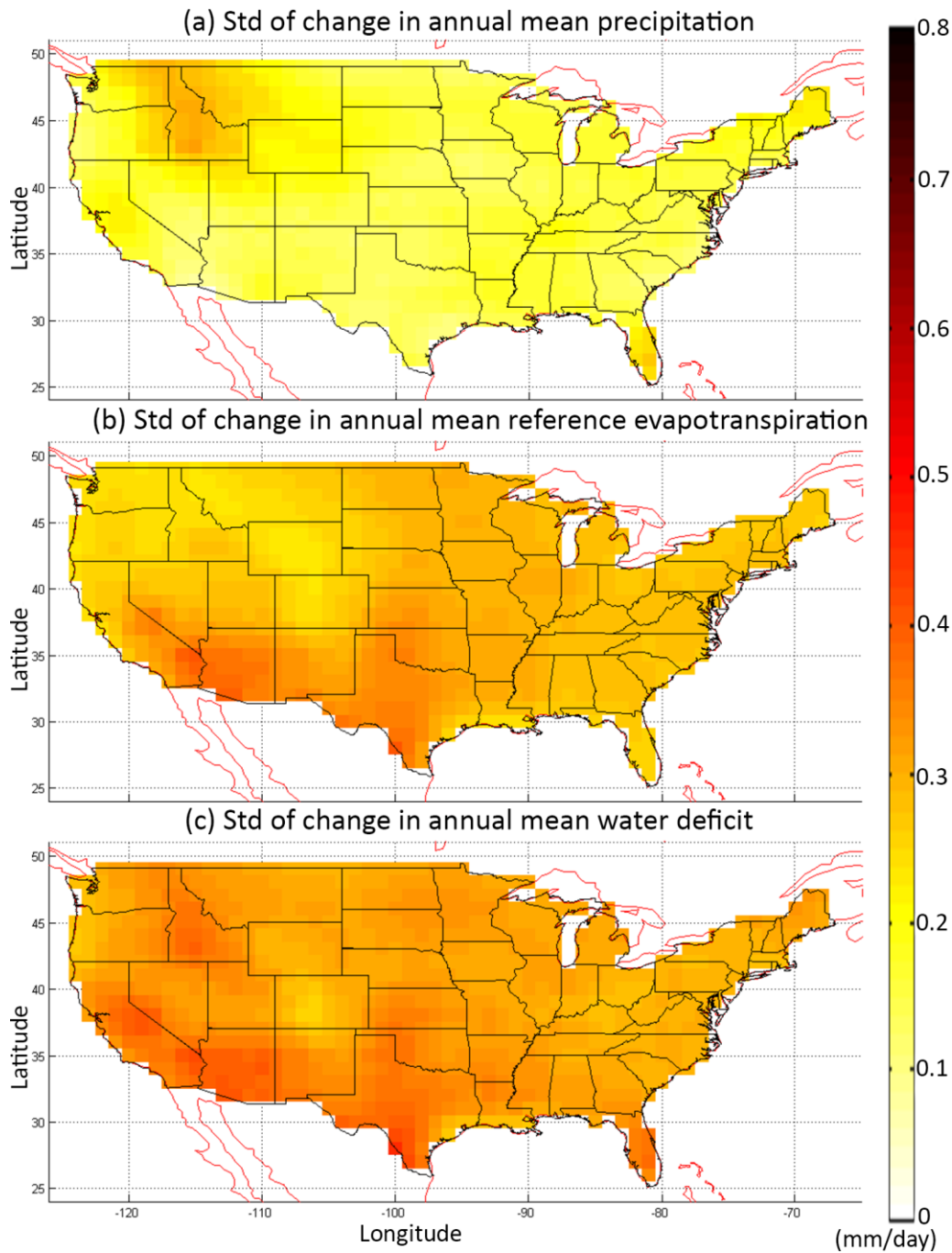
705 **Appendix A: Supplemental figures**



706

707 Fig. S-1 The change in the annual mean (a) P, (b) ET_0 , and (c) $P - ET_0$ over U.S. All units are
708 mm/day and the trend is defined as the average of 2030-2060 minus that of 1950-2005.

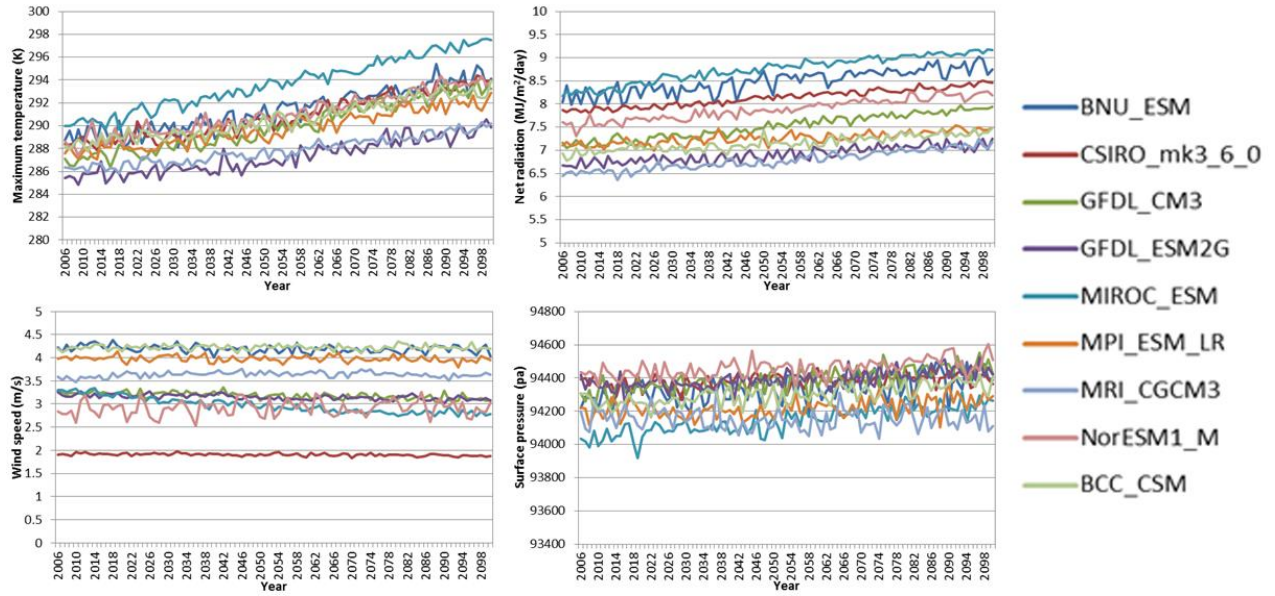
709



710

711 Fig. S-2 The standard deviation of the change in the annual mean (a) P, (b) ET_0 , and (c) $P - ET_0$
 712 over U.S. All units are mm/day and the trend is defined as the average of 2030-2060 minus that
 713 of 1950-2005.

714



715

716 Fig. S-3 Mean maximum temperature, net radiation, wind speed at 2 m surface, and surface
 717 pressure of CMIP5 for future period (RCP 8.5).

718